Graduate School ETD Form 9
(Revised 12/07)

PURDUE UNIVERSITY
GRADUATE SCHOOL
Thesis/Dissertation Acceptance

This is to certify that the thesis/dissertation prepared

By Alexander David Meadows

Entitled
PLANT ERROR COMPENSATION AND JERK CONTROL FOR ADAPTIVE CRUISE CONTROL SYSTEMS

For the degree of Master of Science in Electrical and Computer Engineering

Is approved by the final examining committee:

Lingxi Li
Chair

Yaobin Chen

Glenn Widmann

To the best of my knowledge and as understood by the student in the *Research Integrity and Copyright Disclaimer (Graduate School Form 20)*, this thesis/dissertation adheres to the provisions of Purdue University's "Policy on Integrity in Research" and the use of copyrighted material.

Approved by Major Professor(s): Lingxi Li

Approved by: Brian King 03/19/2012
Head of the Graduate Program Date

Graduate School Form 20
(Revised 9/10)

PURDUE UNIVERSITY
GRADUATE SCHOOL

Research Integrity and Copyright Disclaimer

Title of Thesis/Dissertation:

PLANT ERROR COMPENSATION AND JERK CONTROL FOR ADAPTIVE CRUISE CONTROL SYSTEMS

For the degree of Master of Science in Electrical and Computer Engineering

I certify that in the preparation of this thesis, I have observed the provisions of *Purdue University Executive Memorandum No. C-22,* September 6, 1991, *Policy on Integrity in Research.**

Further, I certify that this work is free of plagiarism and all materials appearing in this thesis/dissertation have been properly quoted and attributed.

I certify that all copyrighted material incorporated into this thesis/dissertation is in compliance with the United States' copyright law and that I have received written permission from the copyright owners for my use of their work, which is beyond the scope of the law. I agree to indemnify and save harmless Purdue University from any and all claims that may be asserted or that may arise from any copyright violation.

Alexander David Meadows

Printed Name and Signature of Candidate

03/20/2012

Date (month/day/year)

*Located at http://www.purdue.edu/policies/pages/teach_res_outreach/c_22.html

PLANT ERROR COMPENSATION AND JERK CONTROL FOR ADAPTIVE CRUISE CONTROL SYSTEMS

A Thesis

Submitted to the Faculty

of

Purdue University

by

Alexander David Meadows

In Partial Fulfillment of the

Requirements for the Degree

of

Master of Science in Electrical and Computer Engineering

May 2012

Purdue University

Indianapolis, Indiana

To my leading ladies: my wife Rachael, and our daughter Fiona.

ACKNOWLEDGMENTS

I would like to recognize the great assistance I have received from my advisor, Dr. Lingxi Li, and my additional committee members, Dr. Glenn Widmann and Dr. Yaobin Chen. Thank you all for your advice, your expertise, and your help.

I further acknowledge the many years of assistance from Sherrie Tucker, above and beyond her duties as department office coordinator. Thanks for all the coffee, cookies, copies, faxes, smiles, laughs, calls, sandwiches, pizzas, emails, reminders, and encouragement.

Finally, I acknowledge the lengthy support and encouragement of friends and family. Thanks for putting up with my antics and peculiarities, for proofing my many documents, and for humoring my engineering discussions. Special thanks to my nuclear and extended families without whose patience I might never have survived.

TABLE OF CONTENTS

Page

LIST OF TABLES

LIST OF FIGURES

SYMBOLS

a	acceleration
a, b	exponential system parameters; the inverse of time constants.
α_n, β_n	the minimum and maximum values, respectively, of a_n.
A_n	constant coefficients of exponential functions in the time domain.
a_n	the ordered coefficients of the characteristic equation.
b_{n-1}	the first computed value in an Routh–Hurwitz array, *see equation* (4.20).
e	exponential constant, natural logarithm base; $\approx 2.71828\ldots$
g	the acceleration due to gravity, $9.8\frac{\mathrm{m}}{\mathrm{s}^2}$
γ, λ	*in this work*, unknown factors which determine $\alpha_n = \gamma \cdot a_n$ and $\beta_n = \lambda \cdot a_n$.
γ_{MUP}	*in this work*, a measure of the maximum uniform percentage change that a system can experience while remaining stable; *see equation* (4.49).
$\in$	is a member of
∞	infinity
K	a constant gain, as in a transfer function.
κ	*in this work*, a combination of a_n useful for determining stability; *see equation* (4.33).
λ_{TOT}	*in this work*, a measure of total parametric instability tolerance; *see equation* (4.47).
m	the order of a transfer function numerator; the number of zeros.
m	mass
$\mathbf{j}$	the imaginary number unit, $\mathbf{j}^2 = -1$

N	the order of a transfer function denominator; the number of poles.
ω	radial frequency; the imaginary magnitude of a complex number.
$\propto$	is proportional to
s	the complex frequency variable, $s = \sigma + \mathbf{j}\omega$
t	time, the variable of the time domain.
τ_n	a time constant; a measure of system responsiveness.
v	velocity
x	position
ξ	*in this work*, the jerk.

ABBREVIATIONS

ACC	adaptive cruise control
DC	direct current, a fixed-voltage system.
ft	feet
LIDAR	*Li*ght *D*irection *A*nd *R*anging
m	meters
mph	Miles per hour
PFE	Partial Fraction Expansion
PID	Proportion, Integral, Derivative
RADAR	*Ra*dio *D*irection *A*nd *R*anging
s	seconds (*Not to be confused with the the symbol s.*)
SID	System Identification; System Identity; System ID

GLOSSARY

Bode Plot The Bode Plot provides a two graphs that describe the frequency response of a transfer function. The first graph shows the magnitude of the response vs. frequency. The second shows the phase shift of the response vs. frequency.

Controller The part of a system which is added to correct the operation of a plant, usually through feedback techniques.

Δv *"Delta vee"* is the difference in velocity. This might be the difference in velocity for one particular vehicle between two times, or it may be the instantaneous difference in velocity between two vehicles.

Feedback The technique of taking a portion of the output of a system and applying it to the input in some combination with the input signal—usually subtraction. If the output is modified by a transfer function before being applied to the input, the feedback is said to be *non-unity feedback*.

Laplace Transform An integral transform from the time domain with variable t to the complex frequency domain with variable $s = \sigma + \mathbf{j}\omega$, for some σ and ω. The integral is defined thus:

$$F(s) = \int_0^\infty f(t)e^{-st}dt$$

Lookup Table	A control system which relies on a matrix of precalculated gain values which are selected by indexing one or more measurable conditions of the system. Also called *gain scheduling*. Such a system can be exceptionally robust, as its parameters are well known. Since no *on-the-fly* calculations are required, it switches and reacts very quickly to changing conditions.
MatLAB	A suite of software produced by Mathworks, Inc. which provides tools for creation and manipulation of matrices, systems of equations and engineering solutions.
Partial Fraction Expansion	A collection of algebraic techniques which separate a ratio of polynomials into a sum of ratio terms having denominators which are all the factors of the original denominator. This is particularly useful when employing linear transformations such as the Laplace transform, as the resultant terms may be transformed independently and often with the use of a table.
PID	*Proportion, Integral, Derivative*; A control system where the error signal is formed as a linear combination of the input, the output, the derivative of the output, and the integral of the output. The design of such a system involves determining the appropriate value of the coefficients of combination—a process called *tuning*.
Plant	The part of a system which is to be controlled, having an input and an output and generally described by a transfer function.
RC filter	A basic passive system which provides a frequency-based modulation of signals which pass through it. It is composed of at least one resistor(R) and one capacitor(C) and is characterized by the product of the value of these components.

Root Locus	A single graph which shows, for a transfer function, the path (*locus of points*)which is followed by the poles as they move to the zeros in the complex plane, as some parameter, usually K, is varied. The N−m poles which do not have associated zeros move to a virtual zero at infinity.
SID	*System Identification*; An order-reduction method involving the approximation of a system's response as a lower-order transfer function. The time constants of this new function then become the identity of the system, *e.g.: a (0.5, 0.002) system...*
Simulink	A programming environment inside MatLAB which provides a graphic user interface for the creation of models and for running simulations.
Summing Junction	A point of intersection of two or more signals which produces an output signal as a combination of the sum of some inputs and the difference of others.
Transfer Function	A mathematical representation of a system in the complex frequency domain as the ratio of two polynomials, $G(s) = \frac{num(s)}{den(s)}$, satisfying the relationship $\frac{Y(s)}{R(s)} = G(s)$ where $Y(s)$ and $R(s)$ are the output and input of the system, respectively. The m roots of the numerator polynomial are referred to as zeros, whereas the N roots of the denominator polynomial are called poles. The roots may be *simple*; having only a real part, or be *complex*; having both a real part and an imaginary part.

Vector — A mathematical construct composed of a magnitude and a direction, occurring in some n-space of $n \geq 2$. A vector may be represented by a magnitude and an angle, $\vec{x} = \sqrt{2}\angle 45°$, or by the lengths projected on the axis of the space, $\vec{x} = [1, 1]$.

ABSTRACT

Meadows, Alexander David. M.S.E.C.E., Purdue University, May 2012. Plant Error Compensation And Jerk Control For Adaptive Cruise Control Systems. Major Professor: Lingxi Li.

Some problems of complex systems are internal to the system whereas other problems exist peripherally; two such problems will be explored in this thesis. First, is the issue of excessive jerk from instantaneous velocity demand changes produced by an adaptive cruise control system. Calculations will be demonstrated and an example control solution will be proposed in Chapter 3. Second, is the issue of a non-perfect plant, called an *uncertain* or *corrupted* plant. In initial control analysis, the adaptive cruise control systems are assumed to have a perfect plant; that is to say, the plant always behaves as commanded. In reality, this is seldom the case. Plant corruption may come from a variation in performance through use or misuse, or from noise or imperfections in the sensor signal data. A model for plant corruption is introduced and methods for analysis and compensation are explored in Chapter 4. To facilitate analysis, Chapter 2 discusses the concept of system identification—an order reduction tool which is employed herein. Adaptive cruise control systems are also discussed with special emphasis on the situations most likely to employ jerk limitation.

1. INTRODUCTION

Before delving into the topics of jerk limitation and plant corruption, it is important to appreciate some of the background information. Specifically, we will investigate the types of systems explored for control and the nature of our dynamic model simulation. We will then discuss some of the analytical techniques used to facilitate solutions.

This work deals specifically with adaptive cruise control(ACC) systems in passenger vehicles. For the purpose of analysis and test, a simulation environment called Simulink is used. Simulink is a part of Mathworks' MatLAB, a matrix-based programming and development environment. The simulation uses mathematical models to predict the behavior of systems from the very simple, like an RC filter, to the very complex, such as, the adaptive cruise control systems we are discussing here. The model used for simulation is the same as was used in previous work by Yao Zhai [1].

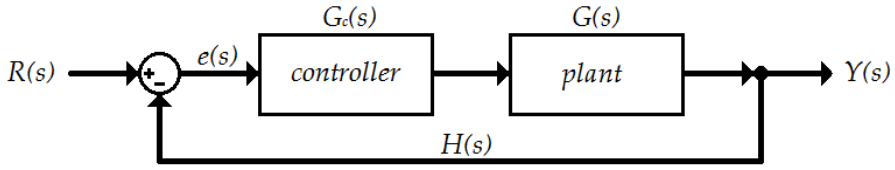

Fig. 1.1. A generic control system with negative feedback.

In control system theory, a controlled system is described as being comprised of a *plant*, a *controller*, and in most cases, a *feedback* loop with a *summing junction.* In a feedback system, the output of the system is compared to the input and an error signal is produced which is used to adjust the process accordingly [2]. In general, a system with negative feedback is a stable choice for control [3]. A generic closed-loop, negative feedback controlled system diagram is depicted in Figure 1.1. This type of control,

Table 1.1
Parts of a generic controlled system.

Term	**Function**
$Y(s)$	System Input
$e(s)$	Error Signal
$G_c(s)$	Controller Transfer Function
$G(s)$	Plant Transfer Function
$H(s)$	Feedback Transfer Function

occurring between the summing junction and the plant is specifically called *cascade compensation* [3]. In such a diagram, the input signal of each functional block enters from the left and the output emerges from the right. Note that such a diagram may represent an abstraction from the true reality of the system—each *plant* or *controller* may be recursively represented by a diagram such as this. The feedback function, $H(s)$, could be any transfer function, but in the most basic diagrams, $H(s) = 1$. A system diagram with a non-unity feedback can be rearranged through various identity properties to produce an equivalent unity feedback system diagram—this is important for analysis techniques which are predicated on such a system [3]. With unity feedback, the error signal input of the controller is simply $e(s) = R(s) - Y(s)$. In other words, the error is formed as the difference between the output and the input. The controller is designed to minimize this error signal. In a simplified example, with a traditional cruise control system, perhaps the car is traveling at 65 mph when the *set* button is pressed. The input of the system becomes the current speed and the error signal is $e(s) = 65 - 65 = 0$. Farther down the road, if the car goes up a hill and its speed decreases to 60 mph, the new error signal is $e(s) = 65 - 60 = +5$, as a result, the control system would issue an acceleration command to the plant, increasing the vehicle speed to match the new set speed. When the car has passed the summit and is going down a hill, its speed increases to 70 mph. The new error signal is

$e(s) = 65 - 70 = -5$, as a result, the control system would generate a deceleration command to the plant, decreasing the vehicle speed to match the new set point.

As this work uses a complex dynamic model, a system identification will be derived to expedite simulation and allow a more fundamental understanding of the interaction of the plant and the controller. Using a system ID model will also allow analytical solutions for the controller. System identification will be described in detail in Chapter 2, along with a demonstration of its application to a part of the model.

1.1 Adaptive Cruise Control Systems

Adaptive cruise control systems have been on the market for many years. The first such system was the *LIDAR*-based "Preview Distance Control" system produced by Mitsubishi Motors Corporation on their 1995 *Diamante* [4]. Most systems were originally available specifically on higher-end vehicles such as the *Volvo S60*, *Audi A8*, and *BMW 7 Series* but are becoming increasingly popular on mid-level cars such as the *Ford Taurus* [5] [6] [7]. Although many complex control systems exist, industry still tends toward the more simple and arguably more reliable *lookup table* for implementation in most systems because they can be defined based on steady state operating conditions which allow transient responses to subside and leave derivatives at zero [8]. Disadvantages of lookup table controllers are that it is computationally intensive, requiring the calculation of a number of linear controllers, and that it has no guarantee of non-linear stability [9]. The inputs are then used to estimate values for operating states falling between those previously calculated on a static test bed [8]. After lookup table control systems, the most logical choice for control is the *PID* controller, or one of its derivatives. Although PID controllers are as familiar to industry as lookup tables, their primary drawback is the necessity to tune the control parameters ahead of time to achieve reasonable functionality. The process of *tuning* is tedious; algorithms exist but do not provide significant reductions in work time.

Adaptive cruise control systems are a further controlled extension of the traditional cruise control systems with which nearly all car owners are familiar. Whereas a standard cruise control system follows an operating point velocity equal to the user-defined set point, an ACC system has an operating point which varies according to the parameters of the system. Referring back to Figure 1.1, the traditional cruise control system is the plant and the adaptive cruise control system is the controller. In such a system, the user selects the initial set point for velocity. Absent perturbations to the car-road system, ACC functions as traditional cruise control. The system may be disturbed in several different ways, such as: driver alertness, road surface conditions, visibility, route curviness, or lead car velocity. Only systems responding to lead car velocities are commercially available, with other disturbance systems the subject of research and development [10] These are the ACC systems considered here. In such a system, when a lead vehicle with lower velocity presents itself in front of the ACC-equipped follow vehicle, the system controls the velocity set point of the follow vehicle until the velocities reach parity and the vehicles have a prescribed separation distance. Figure 1.2 shows a block diagram for a generic ACC system.

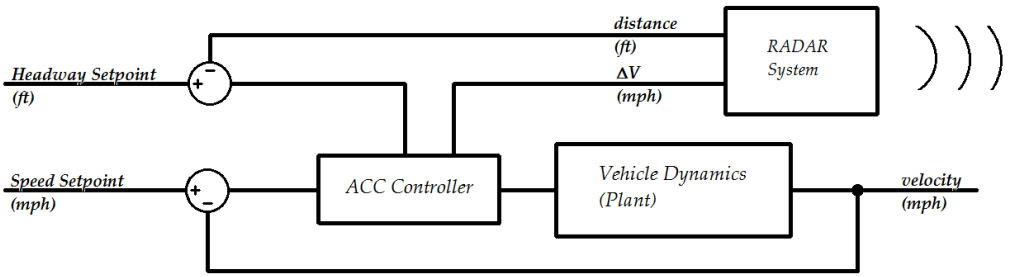

Fig. 1.2. A simplified, generic adaptive cruise control system diagram.

As described, the system must have certain sensors beyond those found in traditional systems. Most important to our discussion is a sensor which detects the relative distance and relative speed of any lead vehicle which is directly in front of the ACC-equipped vehicle. The system most commonly used for this purpose is RADAR. Other

possible systems would include LIDAR or machine vision systems. While the primary purpose of this sensor is to determine the separation distance, the relative velocity combined with the vehicle velocity can also determine the lead vehicle velocity. The ACC system employs certain switching logic which moves between two fundamental modes of operation [1]. In the primary mode, ACC maintains a velocity—much like traditional cruise control. When necessitated by the presence of a slower lead car, the ACC system changes to headway management mode. In this mode, velocity is controlled to maintain the distance relationship with the lead vehicle at the distance set point. At rest, this system provides feedback as to the separation distance and relative speed. An example of follow vehicle distance management is the *two–second rule* we hear from our parents—"stay far enough behind the lead car so that it takes you two seconds to get to where they are now."

Table 1.2
Adaptive cruise control velocity adjustment cases.

1.	*Overtake*: The follow vehicle overtakes a slower lead vehicle initially beyond the range of the detection sensor.
2.	*Cut In*: A vehicle merges into the lane in front of the follow vehicle at a distance less than the maximum range of the distance sensor.
3.	*Lane Departure*: The slower lead vehicle leaves the lane and the follow vehicle resumes the user-initiated set point.
4.	*Velocity Change*: A change in the lead vehicle velocity when the follow car is already in a state of controlled velocity.

Given such a system, the follow vehicle velocity is adjusted under four general cases detailed in Table 1.2. In the first case, the transition is usually gentle, provided the distance sensor has sufficient range capabilities. The second case can result in an unpleasant velocity adjustment, if the Δv between the vehicles is too great, or the

cut-in range is too small. The transition in the third case is generally smooth and is also functionally equivalent to the follow vehicle leaving the lane of the lead vehicle. The final case may result in an increase in velocity or a decrease in velocity.

Jerk limitation will be applied to the system under the auspices of the final case. In the first and third cases, the velocity may easily be controlled to maintain the jerk under a predetermined maximum value, as there are no other constraints on the system. In the second case, there are two constraints, lead velocity and the initial separation. The combination of these two constraints presents a complexity beyond the scope of this analysis. In one case, a car merges in front of the follow car with enough separation and velocity that a control scenario can be applied to bring velocities to parity. In the other case, the car merges in with insufficient separation and velocity to apply control and a collision will occur. With two possible outcomes for the same scenario we are not constrained to a solution. In the final case, we have but one constraint, the lead vehicle velocity. The first case is conceptually equivalent to the fourth case for a lead vehicle initially positioned at the maximum range of the sensor, traveling at the velocity of the follow car, and which immediately executes a velocity change. Presumably, this would be a deceleration event, as an acceleration would remove it from the ACC system's area of effect. Applying jerk limitation in this final case will therefore yield more acceptable results. We will explore some of the requirements and approaches to jerk control in such a circumstance in Chapter 3.

An adaptive cruise control system responds to predetermined perturbations in its environment. In most cases, as mentioned, this has to do with the relative velocities of nearby vehicles. In a purely theoretical system, such as a simulation (even where it is based on real world values), the models behave in an ideal sense. In reality, small variations occur in any signal. In a mechanical signal, such as the power transmitted through a transmission, this may be a small error introduced due to the backlash in a set of gears. In an electrical signal, this may be a small DC offset produced by driving under high voltage electrical wires. In a fluid system, this may be due to expansion or contraction of the fluid or the system components with a change in heat, such as

from winter to summer. In all these cases, one cannot predict the *exact* behavior of the system for every possible environmentally-introduced error. In the abstraction of the system to be considered as a single plant, we must address the variations in the system and determine if we can maintain stability of a system. Such variations in a plant are called plant corruption. This will be explored in Chapter 4 along with a look at the limitations on stability.

1.2 Previous Work

This thesis follows the work produced by Yao Zhai in his thesis entitled "Design of Switching Strategy for Adaptive Cruise Control Under String Stability Constraints" [1]. In his work, Zhai proposed a new control strategy for ACC systems by using a plot of range vs. range-rate. A control system was developed and applied in the dynamic model in Figure 1.3 which simulates vehicle dynamics. Zhai also addressed the issue of string stability in his work. String stability involves analysis of the propagation of error velocities from the lead car to end car in a platoon of vehicles all employing ACC systems. The vehicle dynamics block from Zhai's model is used for simulation in this

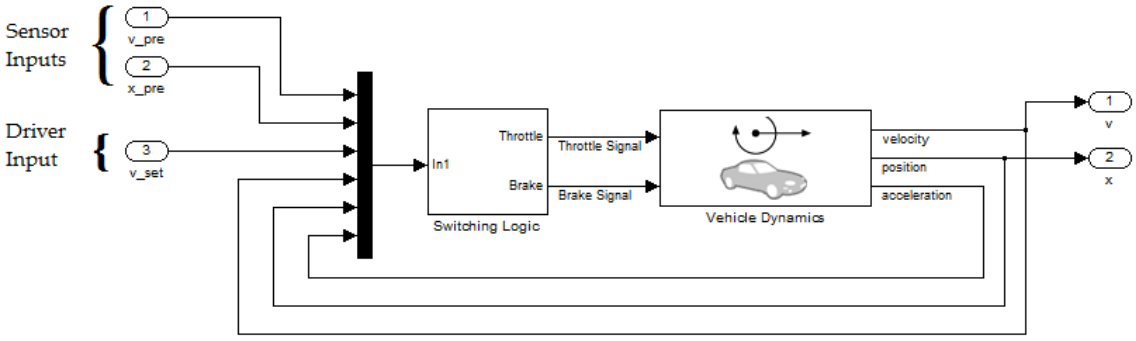

Fig. 1.3. An annotated example of the single vehicle model with ACC control used in Yao Zhai's thesis work [1].

work, applying the same set of parameters to describe the vehicle as in his work. The switching logic block in Figure 1.3 selects different control algorithms based on the

characteristics of the three internal inputs (velocity, position, and acceleration) and the three external inputs (velocity set point, lead vehicle velocity, and lead vehicle position). Based on these inputs, a velocity demand is calculated and the current velocity is subtracted to created a Δv or *dv*. This *dv* is applied to a final *dv*–throttle–brake controller which generates the throttle and brake signals provided as inputs to the vehicle dynamics model [1]. This controller will also be used in this work and is depicted in Figure 1.4. An important feature of this controller is that it guarantees that the ACC system will never apply signals to the throttle and brake commands simultaneously. This practice is mirrored by practical driving skills in modern vehicles

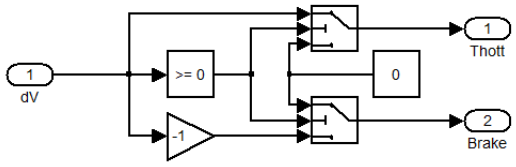

Fig. 1.4. The *dv*–Throttle–Brake controller used in Yao Zhai's thesis work applies positive *dv* to the throttle and applies rectified negative *dv* to the brake with zeros applied otherwise [1].

with one peculiar exception, the original *Saab 92*, employing a two-stroke engine where fuel and lubricating oil are mixed, required drivers to apply the brakes but maintain some throttle to prevent the engine from seizing while going down long hills [11].

For analysis of his model, Zhai determines a representative system identification model. While he calculates the first time constant graphically, he employs the MATLAB System Identification toolbox to find the second time constant. In this paper, the topic of system identification will be explored more thoroughly with surprising results. A graphical, time-domain approach to finding second order complex system models will be described and applied.

1.3 The Dynamic Model

The dynamic model inherited from Yao Zhai is implemented in Mathworks' MATLAB software, specifically in the Simulink modeling suite. The model incorporates various vehicle dynamics such as the specific parameters of the gasoline engine, the differential and the tires. The vehicle model was developed in Japan by Kohakugawa and later used and expanded in his thesis by Yao Zhai [1].

The dynamic vehicle model has two inputs, *throttle* and *brake*. The input is a continuous value between 0 and 1 activating that aspect of the model. As was discussed, control signals are only provided to one input or the other. The primary output of the model is the vehicle velocity. There are also two secondary outputs, which are merely the derivative and integral of the primary output, acceleration and position, respectively. This dynamic model acts as a test bed for control schemes and allows for complex scenarios of multiple vehicles to be tested [1]. The choice to use this model was predicated on previous work in the department [1].

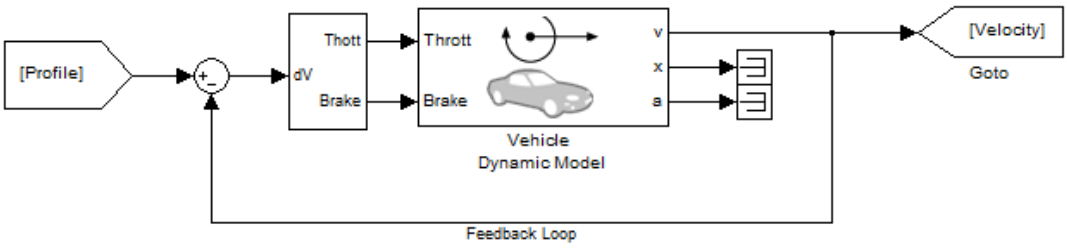

Fig. 1.5. The highest level of the dynamic model, is similar in appearance to the generic control system of Figure 1.1.

The highest level of the dynamic model used in this thesis is shown in Figure 1.5 for comparison to the generic controlled system of Figure 1.1. Figures 1.6 and 1.7 provide a glimpse at successively lower levels of the model to give the reader an idea of the complexity of the dynamic model. An understanding of the specifics of

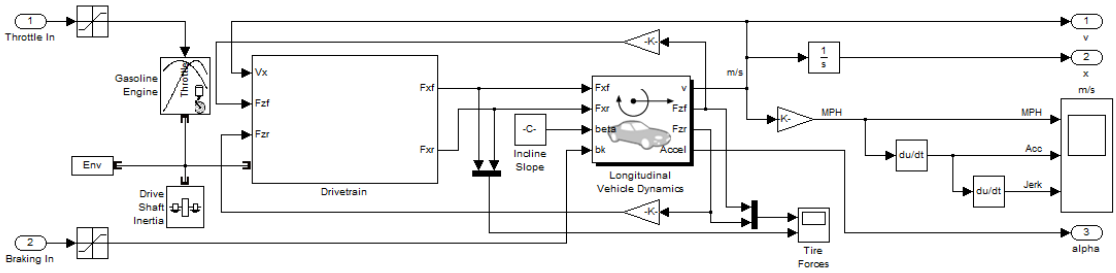

Fig. 1.6. The main layer of the dynamic model shows much greater complexity than a standard transfer function.

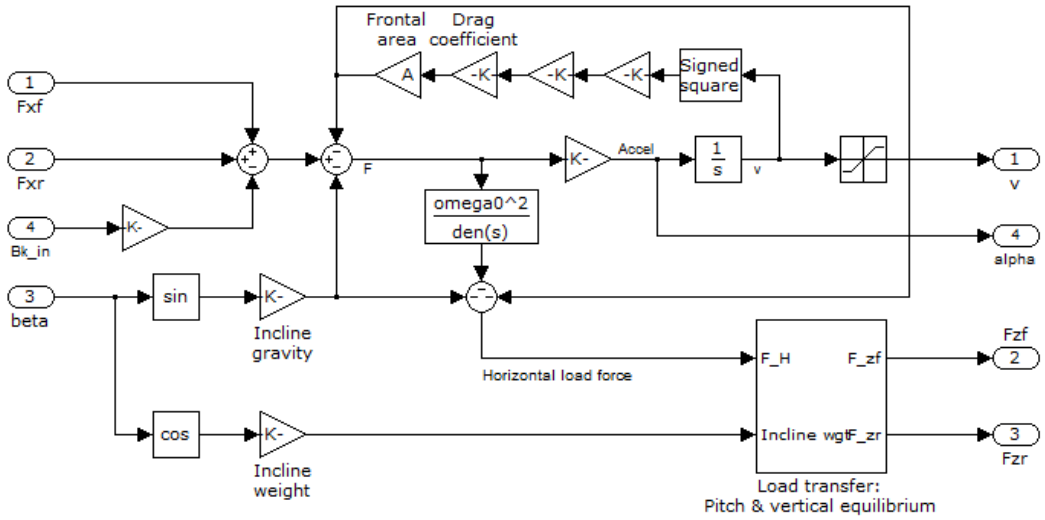

Fig. 1.7. An expanded view of the *Longitudinal Vehicle Dynamics* module of the dynamic model, depicted in Figure 1.6 shows multiple feedback loops.

these models is neither the topic of this thesis, nor required to understand the content presented.

The dynamic model simulates a four–wheel drive vehicle with a gasoline engine. The context of this research is the control of jerk derived from the velocity output of

the model as a result of inputs from an adaptive cruise control system. As such, the method by which those inputs were generated, while interesting, is not germane to the discussion of how they will be processed for jerk limiting. We need only know the shape of the signals to investigate the topic accurately. The dynamic model produces reasonable data for this analysis.

1.4 Chapter Summary

We have discussed a fundamental understanding of what comprises a controlled system. As in Figure 1.1, it is a plant, a controller and a feedback loop. We also have considered that a system such as this may exist inside a particular block of the system diagram. We have explained the broad operational parameters of an adaptive cruise control system and listed the primary disturbances to such a system in Table 1.2. We have discussed the nature of our dynamic model. Finally, we have introduced the three primary topics of discussion for this thesis: System Identification, Jerk Compensation, and Plant Error Compensation.

2. SYSTEM IDENTIFICATION

System identification, often abbreviated as *system ID* or *SID*, is an analysis technique used to provide a simplified mathematical model for a complex system. This technique relies on the fact that the response of a linear system can be represented as a sum of exponential functions of different time constants.

$$y(t) = A_0 + A_1 e^{-\frac{t}{\tau_1}} + A_2 e^{-\frac{t}{\tau_2}} + ... = \sum_{n=0}^{N} A_n e^{-\frac{t}{\tau_n}} \tag{2.1}$$

In creating the system ID, we will choose the A_n terms and the τ_n terms. The A_0 depends on the type of input to the system. Since we will be using a step input, $A_0 = 1$, as will be shown in greater detail below. Our model will be in the complex frequency domain. Using the Laplace transform, it is simple to determine the frequency domain model [3] [12] [13] [14] [15]. In evaluating a signal, we might use foreknowledge to predict the order of the system. For example, in an electrical system containing only a resister and a capacitor we would create only a first order model. If we know the system is more complex, we naturally may predict the necessity of a model of greater order. The process of model generation may be applied recursively to generate successively higher–order models [16]. As we wish to simplify our model, yet maintain a measure of the true response, a second order system will be sufficient. For a second order system with $A_0 = 1$, we will have only the first two exponential terms. It may appear as follows.

$$Y(s) = \frac{1}{s} + \frac{A_1\tau_1}{\tau_1 s + 1} + \frac{A_2\tau_2}{\tau_2 s + 1} \Longrightarrow \frac{(A_1 + A_2)\tau_1\tau_2 s + (A_1\tau_1 + A_2\tau_2)}{(\tau_1 s + 1)(\tau_2 s + 1)} \tag{2.2}$$

Since A_1 and A_2 are arbitrary values, we may simplify by selecting a convenient relationship between the two, $A_2 = -A_1$. Our frequency domain model then simplifies to:

$$Y(s) = A_1 \frac{\tau_1 - \tau_2}{(\tau_1 s + 1)(\tau_2 s + 1)} \tag{2.3}$$

At this point, we recognize that we have an equation with a constant gain and a response which depends on the values of the two time constants τ_1 and τ_2. A final simplification is made by defining $A_1 = \frac{K}{\tau_1 - \tau_2}$, and we arrive at our general second order system ID equation with two simple roots:

$$Y(s) = \frac{K}{(\tau_1 s + 1)(\tau_2 s + 1)} \tag{2.4}$$

At this point, we may freely choose the gain K to be any stable value, since this represents only the addition of an inline amplifier in our design and would not affect its control. Knowing this, we might select an initial value of 1 for K and dispense with any formality in determining the coefficients A_n while determining τ_n. Analytical techniques may be applied later to determine an ideal value for K, such as the Routh–Hurwitz criteria and the root locus—both of which are discussed below [3].

2.1 First Order SID Methods

There are several methods employed to construct a system ID model—both manual and automated. Determination of the time constants can involve a *grey box* process where some functionality of the system is known, or may be applied to a *black box* system where the internal workings are wholly unknown. For manual determination, a direct graphing technique may be applied. MatLAB provides a system ID toolbox which determines time constants and generates models of various types, such as state space models, system ID models, grey-box models and output-error models.

This work uses manual exponential curve matching, to obtain a better understanding of the function of the system. This involves determining the dominant time constant and then subtracting that exponential function from the data and repeating as many times as the order to which we would like to have our model. For the first couple of time constants, this process provides an approximation to the response which is comparable to automated methods. We begin the process by introducing a step input to our dynamic model and recording the output as in Figure 2.1.

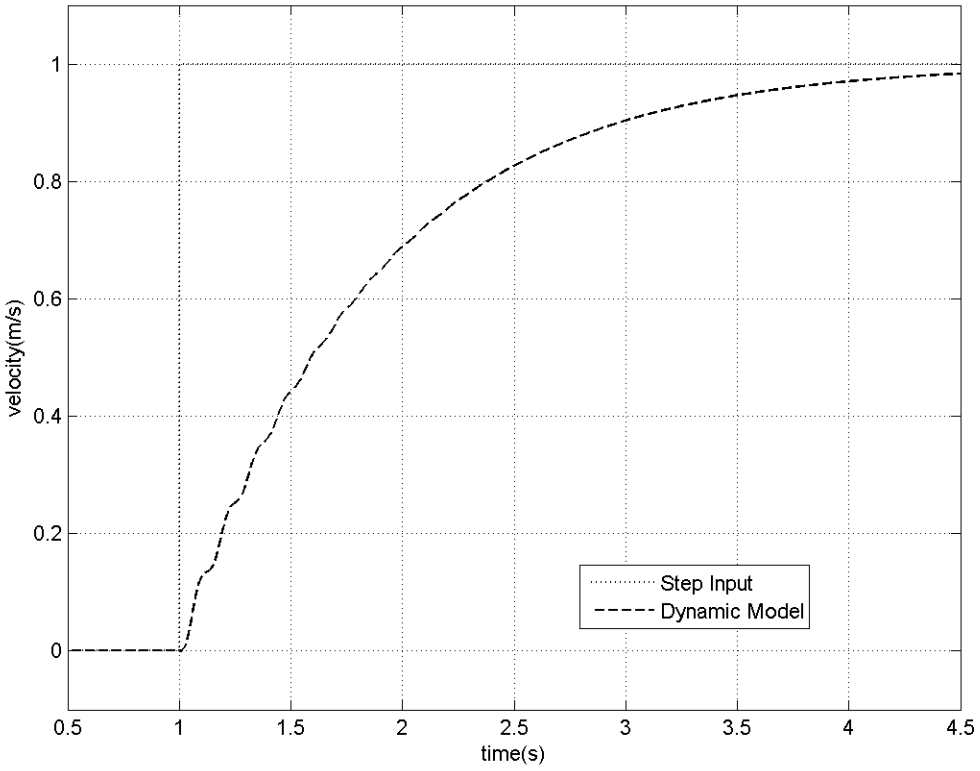

Fig. 2.1. The step response of the dynamic model.

It is the nature of a simple time constant to equal the number of seconds required by a system to change by 63.2% of the applied signal. Consider Equation (2.5). When $t = 0$, $f(0) = 1 - 1 = 0$. After τ seconds have passed, $t = \tau$, $f(\tau) = 1 - e^{-1} = 1 - 0.368 = 0.632$ [1].

$$f(t) = 1 - e^{\frac{-t}{\tau}} \tag{2.5}$$

Knowing this, we measure the first time constant from the plot; subtracting the start time of the step from the time we achieve our target value, a first time constant of 0.864 seconds. Next, we generate data using the following equation with t_0 equal to our delay of one second (note the beginning of the step input) and our $A_1 = 1$.

$$f(t) = 1 - e^{-\frac{(t-t_0)}{(0.864)}} \tag{2.6}$$

For appearances, we have zeroed $f(t)$ before $t = 1$. Again, the leading "1−" term is a result in the time domain of applying a step input in the frequency domain—this will be discussed in greater detail. It is apparent in Figure 2.2 that this function is a close fit to the data, as expected.

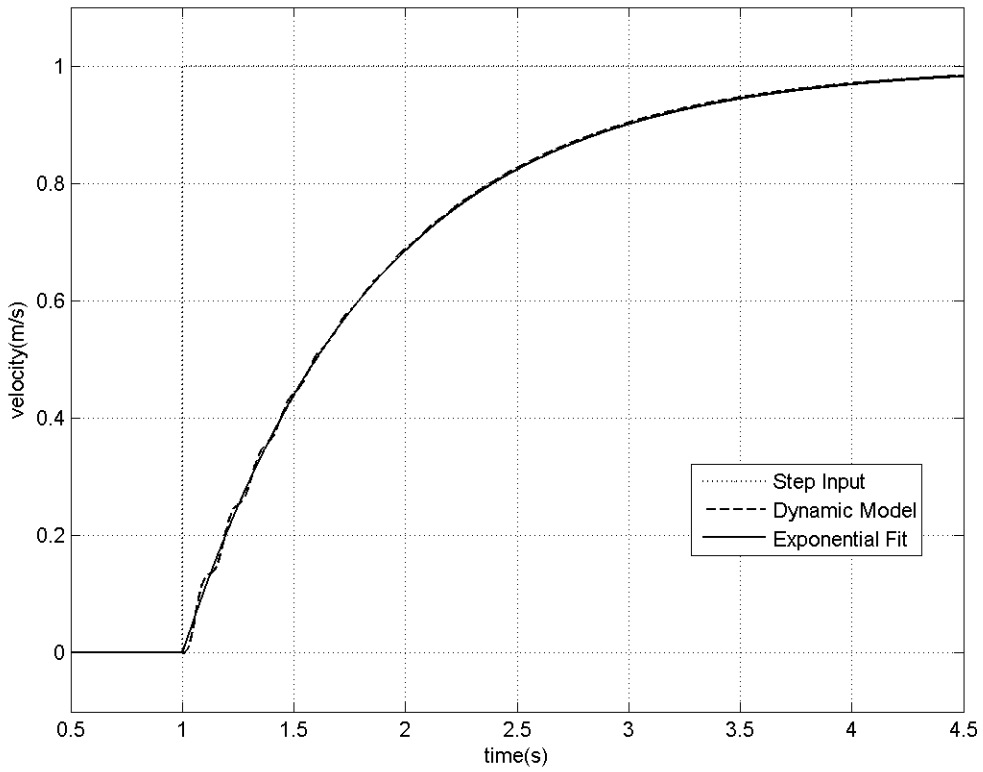

Fig. 2.2. Matching the exponential generated from the first time constant to the dynamic model data shows great similarity.

The next step in the process is to subtract the fitted curve from the data to obtain a difference signal. The difference signal can be a measure of how accurately we have matched the signal and is used in the next step for a second order system ID. We can see in Figure 2.3 that the difference is small, however if we want to quantify the match, something more rigorous is required.

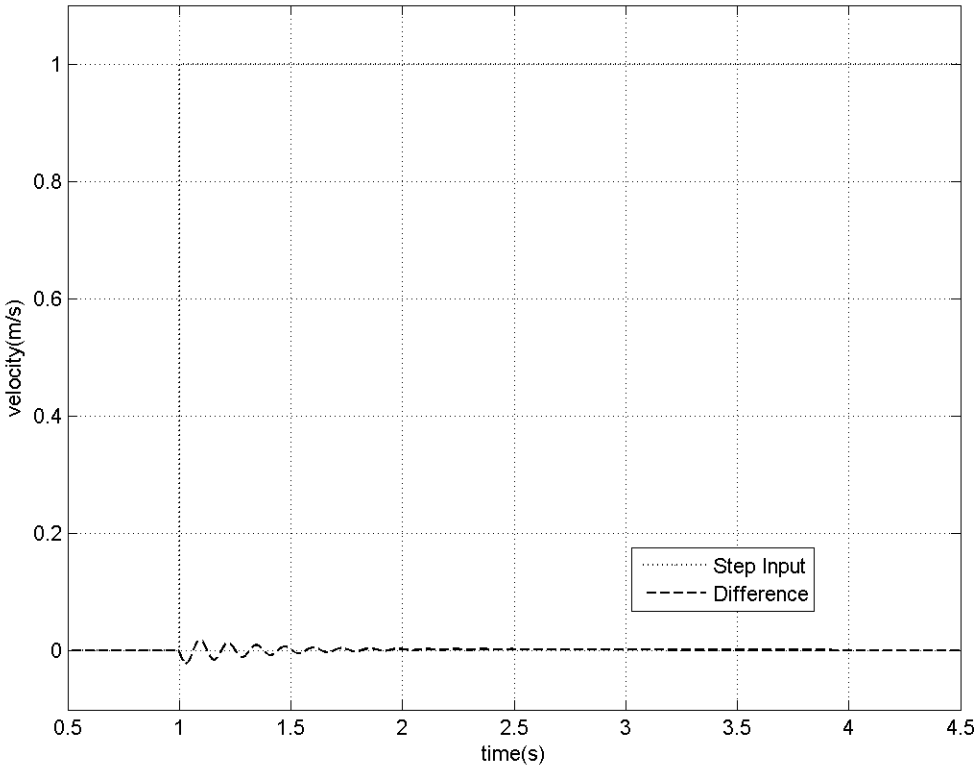

Fig. 2.3. The difference between the dynamic model and the first order system ID.

We may consider that our difference signal represents a vector, $\vec{x}$, where each point in time plots the distance from our signal to the dynamic model data. One method of comparison would be to determine the magnitude of such a vector, called the norm [12]. There are many different norms, but the most commonly used is the 2-norm, also called the *Euclidian* norm [12]. The 2-norm is simply the square root of the inner product of the vector with itself as shown in Equation (2.7). For our difference plot, the formula yields a 2-norm of 0.0637. We can use this method

to evaluate if successive orders of system identification produce signals which better match our data.

$$\| \vec{x} \|_2 := \sqrt{\vec{x}'\vec{x}} = \left(\sum_{i=1}^{n} | x_i |^2 \right)^{1/2} \tag{2.7}$$

2.2 Higher Order SID Methods

If we require a closer fit to the workings of the plant than first order, it will be necessary to perform further analysis on the difference signal [16]. Next, we look at the structure of the data signal in greater detail. Figure 2.4 depicts this difference at an enlarged scale.

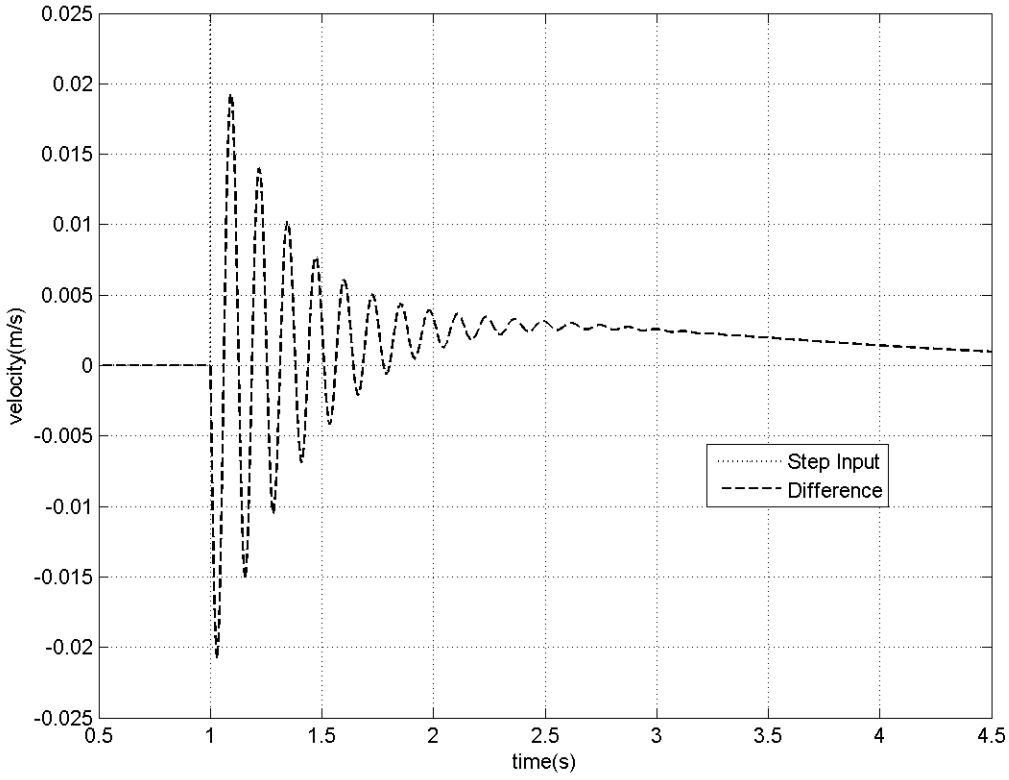

Fig. 2.4. The difference between the dynamic model and the first order system ID, scaled.

Figure 2.4 shows the residual response is of the form of a decaying sinusoid and possibly another function of longer wavelength. Though not visible in this plot, the second function appears to be an over-damped exponential with a smaller amplitude but a larger time constant. The structure of a decaying sinusoid in the time domain becomes a complex double pole in the frequency domain [3] [14]. Equations (2.8) & (2.9) show the time-domain forms of a decaying sinusoid and cosinusoid, respectively, labeled as the second indexed term.

$$f(t) = A_2 e^{-\frac{(t-t_0)}{\tau_2}} \sin\omega(t - t0) \tag{2.8}$$

$$f(t) = A_2 e^{-\frac{(t-t_0)}{\tau_2}} \cos\omega(t - t_0) \tag{2.9}$$

While we expected from previous work to have two real roots as in Equation (2.15), we can see that it is more accurate to use a complex root to account for the decaying oscillations in Figure 2.4 [1]. It can be shown that the supposition of Equation (2.1) is still valid, namely that the function may be reduced to exponentials, by considering that sines and cosines may be expressed as exponentials for complex time constants, where $\theta = \omega t$. [13].

$$\sin\theta = \frac{e^{\mathbf{j}\theta} - e^{-\mathbf{j}\theta}}{2\mathbf{j}} \tag{2.10}$$

$$\cos\theta = \frac{e^{\mathbf{j}\theta} + e^{-\mathbf{j}\theta}}{2} \tag{2.11}$$

Making the necessary substitutions and simplifying, we arrive at a sum of exponentials by substituting Equation (2.11) into Equation (2.9).

$$f(t) = A_2 e^{-\frac{(t-t_0)}{\tau_2}} \left(\frac{1}{2} e^{\mathbf{j}\omega(t-t_0)} - \frac{1}{2} e^{-\mathbf{j}\omega(t-t_0)}\right) \tag{2.12}$$

$$= \frac{A_2}{2} \left(e^{-\frac{(t-t_0)}{\tau_2}} e^{\mathbf{j}\omega(t-t_0)} - e^{-\frac{(t-t_0)}{\tau_2}} e^{-\mathbf{j}\omega(t-t_0)}\right) \tag{2.13}$$

$$= \dot{A}_2 \left(e^{(-\frac{1}{\tau_2}+\mathbf{j}\omega)(t-t_0)} - e^{(-\frac{1}{\tau_2}-\mathbf{j}\omega)(t-t_0)}\right) \tag{2.14}$$

In this case, we have pulled the $\frac{1}{2}$ into A_2, since it remains an arbitrary constant. This exponential form is useful to illustrate that we are still in compliance with our assumptions, but it is needlessly complex for our application. Instead, we return

to the form of Equation (2.9). The practical application of this form involves first determining the frequency ω of the cosinusoid and then the time constant τ_2. Counting approximately 16 half cycles in 1 second, we can estimate $\omega = (16/2)\cdot 2\cdot\pi \approx 50.3$. Through experimental matching, an actual value of 49.965 was determined. Further, imagining a decaying exponential bounding the data and working similarly, the 63.2% decay time is estimated at 0.3s. Again, experimental matching determines the actual value at 0.394s. With the subtraction of the sinusoid term in Figure 2.5, a marked improvement is shown. What is left is another decaying sinusoid and some other longer time constant contribution. Our 2-norm value for this data is 0.03049. At this point, the goal of finding the parameters of a second order system ID is achieved and like a great artist, we must know when to stop. Common convention in modeling is to create a model which is sufficiently complicated to provide adequate data and no more complicated [15]. One measure for the necessary complexity in modeling a system is to consider the degrees of freedom minus the constraints [15]. Our dynamic model of Figure 1.5 has only two inputs, throttle and brake, suggesting a second order model as a primary goal in our system identification.

To determine experimentally, the best fit values for τ_2 and ω, a space is defined, the 2n-b-ω space. For compactness in subsequent formulae and by convention, we define $b = \frac{1}{\tau_2}$ [3] [14]. In this space, we can plot points which represent the 2-norm of the difference of our system ID model from the dynamic model data. These points form a surface as shown in Figure 2.6 plotting 50451 values at a resolution of 0.01. The general shape is a paraboloid. To find the best fit for our second order model, we find the minimum of the surface. High frequency noise in the original plot makes it difficult to appreciate the overall shape. This is alleviated by running ten successive passes of a 3 by 3 gaussian low-pass filter to smooth the image for display purposes [17].

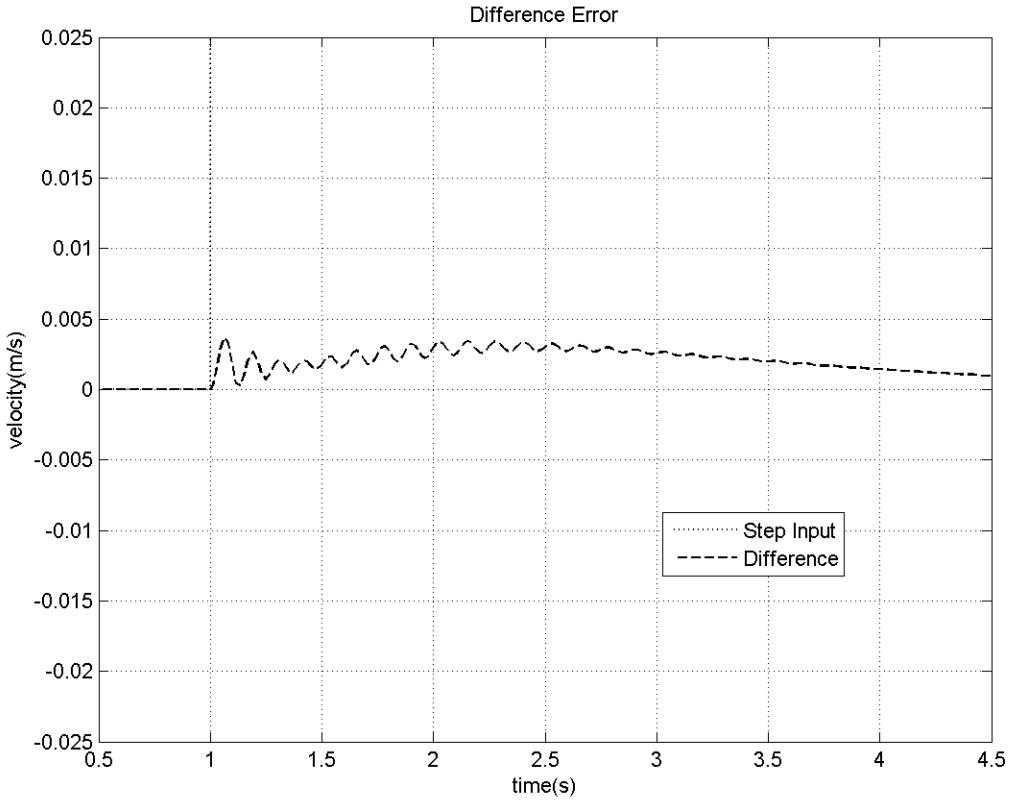

Fig. 2.5. The difference between the dynamic model and the second order system IDs, scaled.

2.3 The SID Transfer Function

To use our system ID in simulation and to perform analysis on it, we must determine the *transfer function*; the complex frequency plane representation of the system. We can determine it from the time-domain response. For compactness, we make the substitutions, $a = \frac{1}{\tau_1}$ and $b = \frac{1}{\tau_2}$. The first term is an artifact of the input signal and is omitted. All the terms are left positive since any required polarity will be explicit in the constants and it is assumed that $t = t - t_0$ for clarity. In the convention of system engineers, the time domain transfer function is labeled as $\mathtt{g(t)}$ and the frequency

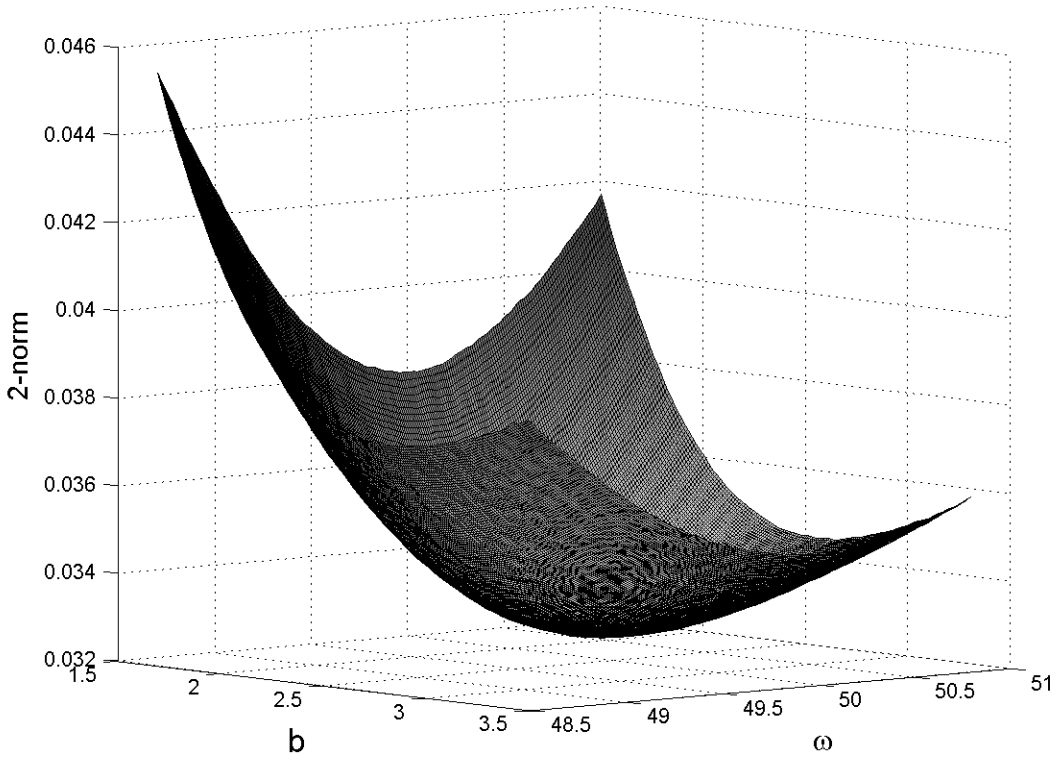

Fig. 2.6. The 2n-b-ω space with 10x Gaussian filtering shows a paraboloid function.

domain equivalent as G(s). Initially, the function is left as a generic, second-order system with one purely-real and one complex pole, as in Equation (2.15).

$$\mathrm{g}(t) = A_1 e^{-at} + A_2 e^{-bt} \cos \omega t \tag{2.15}$$

To derive the specific transfer function in the complex frequency domain, we apply the Laplace transform term-by-term using a lookup table [3]. This yields the sum of terms in Equation (2.16) which is the *partial fraction expansion* of the system's transfer function.

$$G(s) = A_1 \frac{1}{s+a} + A_2 \frac{s+b}{(s+b)^2 + \omega^2} \tag{2.16}$$

Collecting terms and simplifying generates Equation (2.17).

$$G(s) = \frac{[A_1 + A_2]s^2 + [A_2 \cdot a + b(2A_1 + A_2)]s + [A_1(b^2 + \omega^2) + A_2(a \cdot b)]}{(s + a)((s + b)^2 + \omega^2)} \tag{2.17}$$

Great simplification occurs when we choose the relationship (as above) that $A_2 = -A_1$. There may exist numerous different models that would fit the data; this simplification merely selects a subset of those possible models for which these A parameters have the prescribed relationship. The substitution and some simplification leaves us with Equation (2.18).

$$G(s) = (A_1(b - a)\frac{s + (\frac{b^2 - a \cdot b + \omega^2}{b - a})}{(s + a)((s + b)^2 + \omega^2)} \tag{2.18}$$

Just as in Equation (2.15), we will replace the constant gain term with $K = A_1(b - a) = A_1\frac{\tau_1 - \tau_2}{\tau_1 \tau_2}$. This final substitution yields the generic second order system ID transfer function with one complex pole, Equation (2.19).

$$G(s) = K \cdot \frac{s + (\frac{b^2 - a \cdot b + \omega^2}{b - a})}{(s + a)((s + b)^2 + \omega^2)} \tag{2.19}$$

Table 2.1 lists the actual parameters determined for the acceleration system, and Equation (2.20) shows the specific transfer function for our acceleration system. Finally, Figure 2.7 shows the response of our transfer function to a step input, compared to the response of the dynamic model.

Table 2.1
Second order system ID parameters for acceleration system.

a	1.157	τ_1	0.864
b	2.54	τ_2	0.394
ω	49.9	K	1.383

$$G(s) = 1.383 \cdot \frac{s + 1803}{(s + 1.157)((s + 2.54)^2 + (49.9)^2)} \tag{2.20}$$

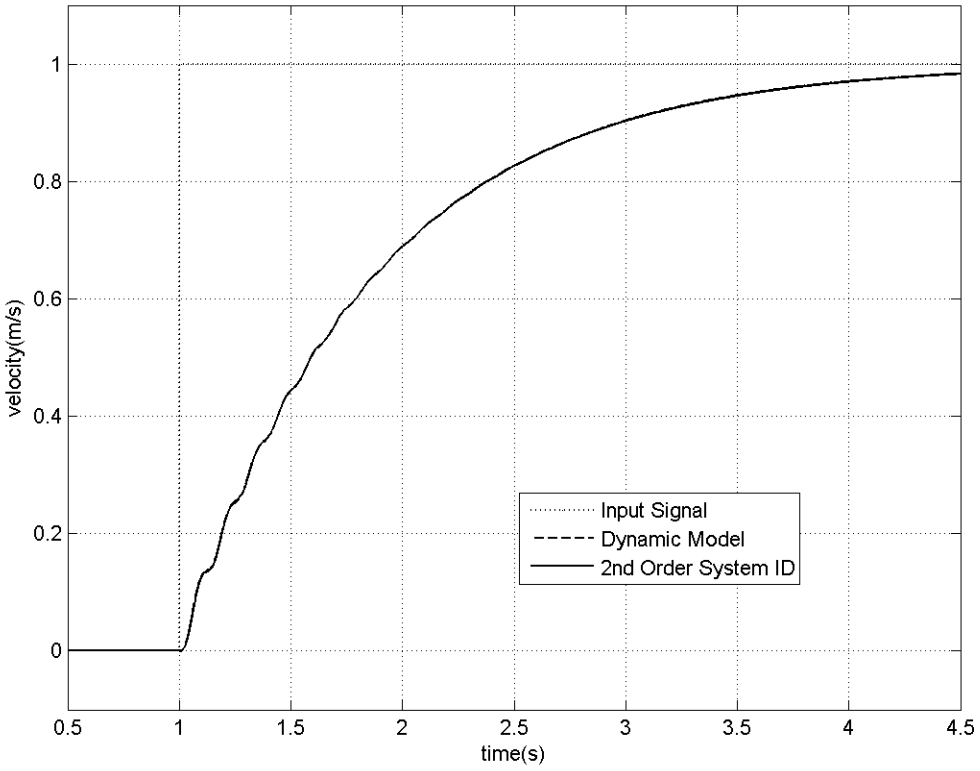

Fig. 2.7. The second order system ID with one complex pole is a very close fit to the dynamic model data.

2.4 System Identification in Complex Systems

For a more complex system, the response to a step up may be different from that of a step down. This is the case particularly if different systems are responsible for actuation in the plant, such as in automobiles. The acceleration system in most automobiles is comprised of the internal combustion engine, the transmission, the trans–axles and the wheels. The braking system is comprised of the wheels, the brake shoes, the brake cylinders, and the master cylinder. This second system has a much faster response, since it must overcome the velocity of the vehicle very quickly to achieve a very short stopping distance. Because the two systems will never be

applied simutaneously, they are decoupled from each other and each may be addressed independently. By applying the same techniques used for the acceleration system, I determined a second order system ID function for the braking system. The parameters are listed in Table 2.2 and the transfer function is listed in Equation (2.21). In this instance, the simplification applied before, $A_2 = -A_1$, did not result in a reasonable response and so both were set equal to 1. As a result, the system ID has a pair of complex zeros.

Table 2.2
Second order system ID parameters for braking system.

a	4.41	τ_1	0.227
b	5.60	τ_2	0.179
ω	50.65	K	8.735

$$G(s) = 8.735 \cdot \frac{s^2 + 10.6s + 1310}{(s + 4.41)((s + 5.60)^2 + (50.65)^2)} \tag{2.21}$$

The response of the second order system ID function is compared to the dynamic model in Figure 2.8. The second order difference is shown in Figure 2.9. Having collected a system ID for both the acceleration and braking systems, it may be interesting to see how the model compares to both. This is plotted in Figure 2.10.

There are some challenges in trying to represent the system with a system ID approximation. In practice, if the response to each case is important to the control design, it is most efficacious to consider two separate system ID approximations independently. In the case of our system, we look at one approximation of the braking system and one approximation of the acceleration system. Figure 2.10 shows a plot of the total response of the dynamic model to a step acceleration at 1s and a step deceleration at 11s. Plotted with the response of the dynamic model are the responses

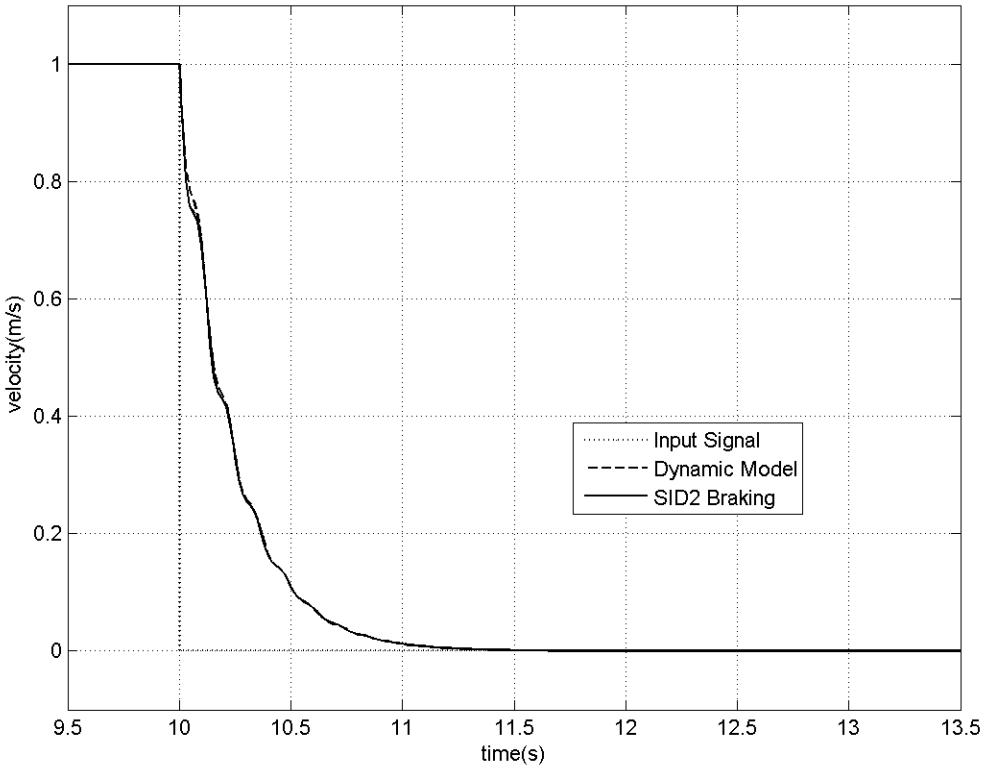

Fig. 2.8. The second order system ID fits the dynamic model data reasonably well.

of the acceleration SID2 and the braking SID2 introduced above. Notice that each system ID is accurate only in the case of the operation for which it was designed.

2.5 Chapter Summary

We have now explored the method of system identification and its application to a part of the problem at hand. The system ID is an important tool in system analysis. For a given model of great complexity, the system ID can provide a large reduction in order, even a selection of order for analysis. For an unknown system, a model of a given order may be created by analysis of recorded data. The successful creation of a

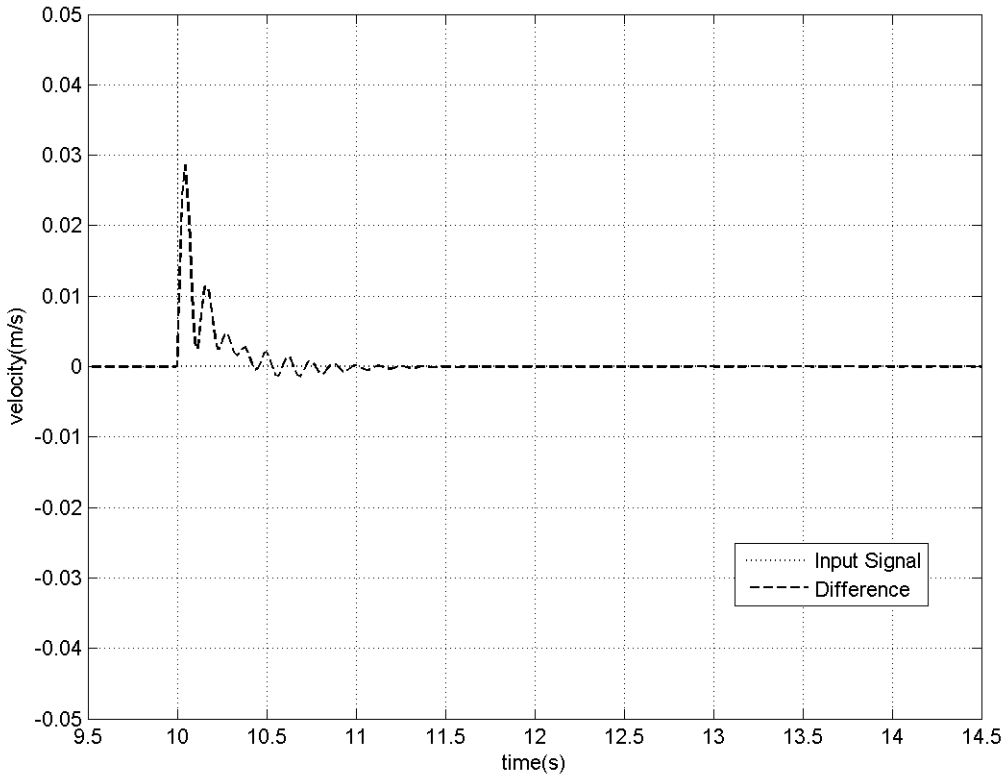

Fig. 2.9. The second order system ID error for the deceleration system, scaled.

system ID model depends on proper determination of time constants and gain. There are automated techniques that will yield good results for time constants. There are also manual curve-fitting techniques that yield reliable results.

In subsequent chapters, we will use the system ID model derived here for analysis and compensation of the jerk in Chapter 3. We also will use this transfer function to explore plant corruption through the method of uncertain parameters in Chapter 4.

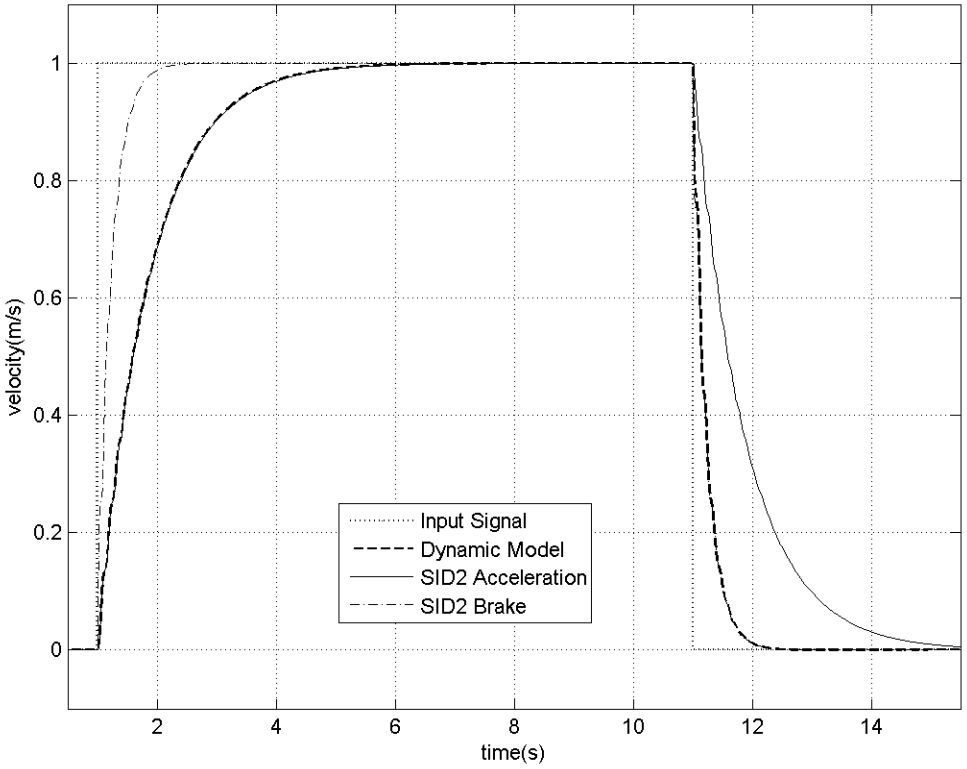

Fig. 2.10. When a plant has two distinct transition characteristics, they can be analyzed as separate system ID functions.

3. JERK COMPENSATION

Humans do not have the capacity to sense velocity. The sensation of walking down the aisle in a bus and walking down the aisle in a plane feel equivalent to walking down the street—yet the relative velocities between these situations are quite high. What is perceived is acceleration—the rate of change of velocity. Acceleration is measured in g, $\frac{\mathrm{m}}{\mathrm{s}^2}$, $\frac{\mathrm{ft}}{\mathrm{s}^2}$, or $\frac{\mathrm{mph}}{\mathrm{s}}$.

Without special equipment used by fighter pilots and stunt pilots, a forward acceleration of $\approx 17g$ and a negative acceleration of $\approx 12g$ of negative acceleration without losing consciousness [18]. This magnitude of acceleration force is seldom experienced in an automobile. The acceleration record for one quarter mile was set by a drag racer at 4.801 seconds, which is equivalent to only $3.6g$ [19] A study from the University of California, Berkeley suggests that a comfortable limit for acceleration in a vehicle is $\pm 2\frac{\mathrm{m}}{\mathrm{s}^2}$, approximately $\pm 4.5\frac{\mathrm{mph}}{\mathrm{s}}$ or $\pm 0.2g$ [20].

The absolute magnitude of acceleration is not the only concern when it comes to comfort, however. We must also consider the smoothness of the acceleration. When the rate of change of the acceleration is smooth, the sensation is comfortable; when the rate of change is choppy, the sensation is uncomfortable. Examples of these are the smooth acceleration of a train from the station to cruising speed vs. the sudden deceleration from braking to avoid a collision. The rate of change of acceleration is aptly named the 'jerk' and is denoted in this paper as ξ [8].

$$v = \frac{\mathrm{d}x}{\mathrm{d}t} \tag{3.1}$$

$$a = \frac{\mathrm{d}v}{\mathrm{d}t} = \frac{\mathrm{d}^2x}{\mathrm{d}t^2} \tag{3.2}$$

$$\xi = \frac{\mathrm{d}a}{\mathrm{d}t} = \frac{\mathrm{d}^2v}{\mathrm{d}t^2} = \frac{\mathrm{d}^3x}{\mathrm{d}t^3} \tag{3.3}$$

Equations (3.1) through (3.3) show convenient derivations for the jerk. The same University of California, Berkeley study suggests that a comfortable limit for jerk is $\pm 5\frac{\mathrm{m}}{\mathrm{s}^3}$, which is equivalently $\pm 11.2\frac{\mathrm{mph}}{\mathrm{s}^2}$ or $\pm 0.5\frac{g}{\mathrm{s}}$ [20]. Anyone who gets motion sick in a car is familiar with the jerk. The sensations produced by going around a sharp turn or suddenly descending a hill are associated with a lateral jerk as compared to the direction of travel. For the ACC system, we are most concerned with the jerk which occurs in the same direction as the travel of the car, but the possibility for discomfort is similar.

As discussed in Chapter 1, it is of interest to approach the control of jerk during the fourth case of Table 1.2, *velocity change*. In the context of this situation, the follow car, equipped with the active ACC system, is initially traveling at some velocity v_0 at t_0. The lead car is also initially traveling at v_0, thus the system is in equilibrium with a parity in velocity between lead and follow vehicles. At some time, $t_1 > t_0$, the lead car executes a velocity change to some new velocity, $v_0 + \Delta v$.

$$v_{follow} = v_0 \tag{3.4}$$

$$v_{lead} = v_0 + \Delta v \tag{3.5}$$

$$v_{lead} - v_{follow} = \Delta v \tag{3.6}$$

This Δv can be measured directly by the ACC system's sensor, such as radar or ultrasonic range finding systems. If x_1 and x_2 are distance measurements at successive times t_1 and t_2, then Δv may be calculated from either of the following formulae.

$$\Delta v = \frac{x_2 - x_1}{t_2 - t_1} = \frac{\Delta x}{\Delta t} \tag{3.7}$$

$$\Delta v = \lim_{\Delta t \to 0} \frac{\Delta x}{\Delta t} = \frac{dx}{dt} \tag{3.8}$$

Although the lead car would actually follow some curving change in velocity, just like our model was demonstrated to do in response to a step change, it is assumed that the change in velocity results in a step change in Δv. This presents a *worst case scenario* for velocity demand violating our jerk limits under normal circumstances. It is this velocity demand which forms the step change input to the ACC system.

3.1 The Ideal "Constant" Jerk Response

In design of a system, it is important to start with some goal in mind. Our goal is to limit the jerk to no more than $\pm 5\frac{\mathrm{m}}{\mathrm{s}^3}$, but let us consider the shape of such a signal [20]. A better understanding is obtained by considering the response of a system which always has a jerk of this magnitude or zero, such as in Figure 3.1. Compare this to the velocity profile of a system with constant acceleration of $\pm 2\frac{\mathrm{m}}{\mathrm{s}^2}$

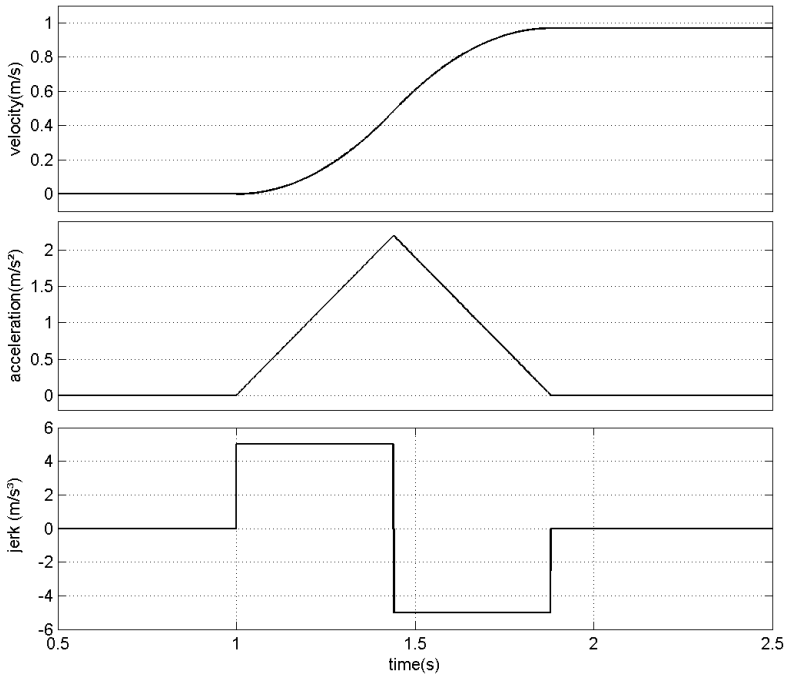

Fig. 3.1. The velocity, acceleration and jerk profiles of an ideal constant jerk system.

as in Figure 3.2. You can see that a controlled jerk presents as a rounded shape in the corners in the velocity plot. The constant acceleration provides a fixed slope in the velocity plot. Our objective in applying control to the jerk will be to cause the sharp transitions as in the constant acceleration system to be rounded out to a closer approximation of the shape of the constant jerk system, while maintaining the

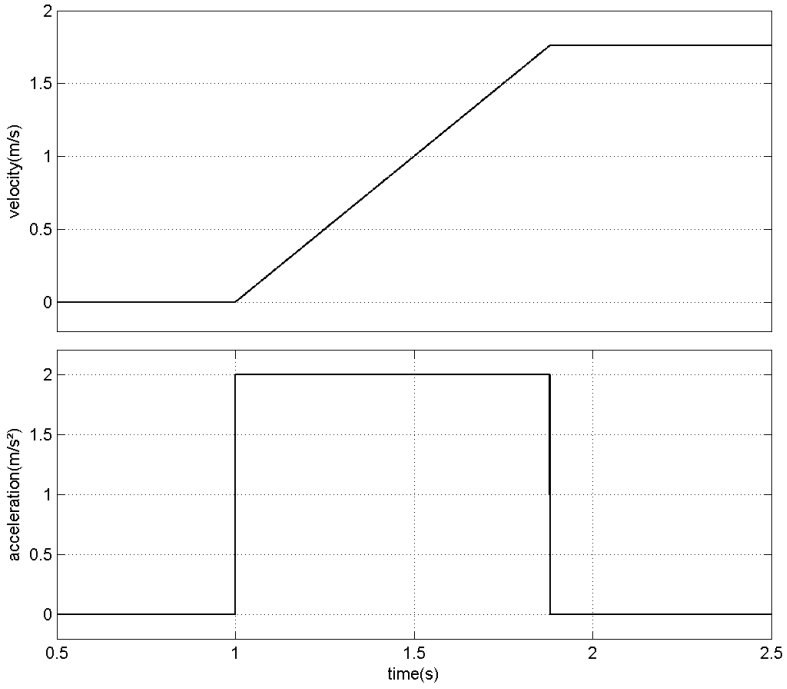

Fig. 3.2. The velocity and acceleration profiles of an ideal constant acceleration system.

maximum slope of the constant acceleration system. The response of the plant will then be this value at most.

Parallel work into this type of signal is found as the goal of motor controllers, many of which are designed with a constant jerk system for determining the velocity profile. An advantage that motor controllers have over ACC systems, however, is knowledge of the future state of the motor. The motor is restricted to one degree of freedom and often the final position is known at the time of the velocity command. An ACC system can know the current velocity demand, but cannot predict the end position of the vehicle. In the case of the motor controller, knowing the end point of position, the maximum permissible jerk, and the maximum velocity of the motor, an acceleration profile is generated. The acceleration would present either as a triangle, or as a rhombus—depending on the maximum rate of acceleration for the motor and the rotation distance of the demand.

3.2 Derivations of a Jerk Compensation Network

Design of a compensation system can be most readily accomplished using one of two analytical techniques, the Bode Plot and the Root Locus. The Bode Plot provides two graphs, a plot of the system gain vs. frequency and a plot of the system phase shift vs. frequency. The Root Locus is a single graph which shows, for a transfer function, the path (*locus of points*) which is followed by the poles as they move to the zeros in the complex plane, as some parameter, usually K, is varied. Examples of these plots for the acceleration and braking system identification models are in Appendix B.

To prevent jerk in the output of the plant, we must prevent signals that would create jerk. Once a signal that creates jerk has been applied, it is too late to prevent the jerk. Therefore, we must address the shape of the applied velocity profile. We accomplish this by placing a compensator between the demand and the plant. This type of compensation is called *input compensation* [3]. The system arrangement is shown in Figure 3.3. The dynamics of our compensator must provide a slow transition to acceleration and velocity.

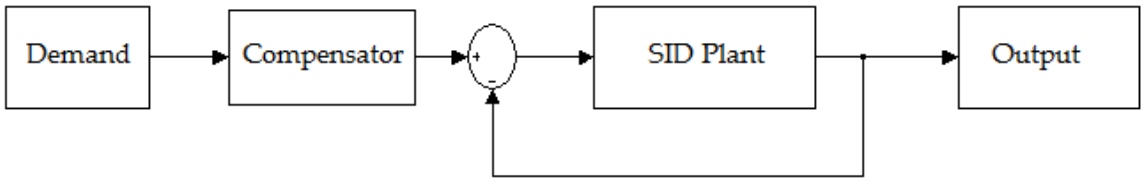

Fig. 3.3. The input compensator modifies the properties of the demand signal to control the jerk in the output.

There are three potentially viable approaches to accomplish our goal. The first is the analytical solution. A transfer function that provides the desired response forms the compensator. The second approach is the dynamic solution. A complex arrangement of functional blocks, mathematical comparisons, and mathematical operations which dynamically calculates the response forms the compensator. A fast transition

in any signal is associated with a high frequency component of the signal [13]. Our goal may therefore be accomplished with the use of a low pass filter [14]. The final approach is a blending of the two. We will now investigate each of these solutions.

Table 3.1 presents the design requirements for the jerk-limiting input compensator. Goals 1 and 2 are readily achievable though analysis but provide conflicting results with goals 3 and 4. A higher multiplicity of filter will limit the maximum jerk, but introduces a longer delay. As the responsiveness goes up, so to does the maximum acceleration. Goal 5 requires careful consideration and will dictate what can be achieved for the other goals.

Table 3.1
Design goals for the jerk-limiting input compensator.

1.	Limit the Jerk to $\pm 5 \frac{\mathrm{m}}{\mathrm{s}^3}$.
2.	Limit the acceleration to $\pm 2 \frac{\mathrm{m}}{\mathrm{s}^2}$.
3.	Minimize the delay.
4.	Maximize the responsiveness.
5.	Provide control for an appropriate step magnitude.

3.2.1 An Analytical Solution

The primary merits of the analytical solution are the simplicity of construction and analysis. For a low pass filter on the input, an arrangement of resistors and capacitors can be used to form a simple low pass filter. In proper arrangement, a filter of n^{th} order will have a transfer function as in Equation (3.9).

$$G_c(s) = \frac{\left(\frac{1}{RC}\right)^{\mathrm{n}}}{\left(s + \frac{1}{RC}\right)^{\mathrm{n}}} \tag{3.9}$$

Table 3.2
The response of the acceleration system to various step input magnitudes with filters of n multiplicity and -3db point at $5hz$.

		Step Magnitude ($\frac{\text{m}}{\text{s}}$)			
n	Metric	0.45	4.5	13.4	Delay (s)
1	accel.	0.58	5.81	17.26	1.16
	jerk	7.33	73.76	221.28	
5	accel.	0.32	3.23	9.70	1.73
	jerk	0.66	5.86	16.54	
9	accel.	0.25	2.59	7.73	1.83
	jerk	0.34	3.83	9.97	

accel. in $\frac{\text{m}}{\text{s}^2}$*; jerk in* $\frac{\text{m}}{\text{s}^3}$

Such a filter is simple and well understood. The price of simplicity is a gradual roll-off of response at a rate of n·20dB per decade after the -3dB point of the filter compared to active filters. Also, this filter is passive, the amplitude of the output depends on the input, as do the amplitude of successive derivatives. Thus the degree to which the jerk and acceleration are limited by such a filter depends on the size of the step change in the velocity demand. The -3dB point is set by the combination of resistor and capacitor values selected. For purposes of comparison, we initially choose a value of 5hz for the product. Table 3.2 shows a comparison of the maximum acceleration of the acceleration system in response to various magnitudes of step inputs filtered through RC filters of several multiplicities.

It should be clear from the table that the response of each filter is proportional to the magnitude of the input. Also, the higher-order filters provide more limiting for a given input. In the final column of the table, we see another trade-off which must be considered. The higher-order filters have a longer delay in the time required to reach 10% of the applied signal. Now we consider the location of the n-pole in Table 3.3.

Table 3.3
The response of the acceleration system to various step input magnitudes with filters of multiplicity 5 and -3db points at several locations.

		Step Magnitude ($\frac{\text{m}}{\text{s}}$)			
p_c	Metric	0.45	4.5	13.4	Delay (s)
0.5	accel.	0.04	0.43	1.30	5.27
	jerk	0.02	0.12	0.34	
1	accel.	0.08	0.85	2.56	2.80
	jerk	0.05	0.41	1.17	
2	accel.	0.16	1.60	4.83	1.54
	jerk	0.14	1.37	3.99	

accel. in $\frac{\text{m}}{\text{s}^2}$*; jerk in* $\frac{\text{m}}{\text{s}^3}$

Clearly, there is a relationship between the pole location and the performance of the filter. A pole closer to the origin has better limiting, but a longer delay. A linear relationship exists between the magnitude of the step signal and the output of the acceleration system. Therefore, choices must be made in the design of the compensator. We therefore consider the normal operating parameters of an ACC system. Under normal operating conditions, we can take our requirement directly from the US interstate highway system. Some interstate highways have both a minimum and maximum speed. While not all states have the same speed limits, the ranges are close enough that we may take the difference of the minimum and maximum of nearly any example to get a good basis for a potential step change. The most common speed limit on interstate highways in the US is 70mph with an associated minimum of 40mph. This yields a step change of 30mph for an ACC set at the maximum velocity overtaking a vehicle at the minimum velocity. In SI units, this is $\approx 13.4\frac{\text{m}}{\text{s}}$. Several combinations of pole location and multiplicity may give the parameters we require. Table 3.4 shows a comparison of some such filters.

Table 3.4
The response of the acceleration system to a 13.4$\frac{\text{m}}{\text{s}}$ step magnitude with filters of various multiplicity and -3db points at several locations.

		Multiplicity (n)		
p_c	Metric	5	9	13
0.75	accel.	1.94	1.39	1.14
	jerk	0.70	0.32	0.21
1	accel.	2.56	1.85	1.52
	jerk	1.17	0.58	0.37
1.3	accel.	3.27	2.39	1.97
	jerk	1.91	0.91	0.58

accel. in $\frac{\text{m}}{\text{s}^2}$*; jerk in* $\frac{\text{m}}{\text{s}^3}$

Examining the diagonal values, it is clear that we can find several combinations providing the response we require. Minimizing n, reduces the number of components, so we might choose a filter with $n = 5$ and $p_c = 0.75$, the response of which is shown in Figure 3.4. The acceleration system with this filter takes 12.6 seconds to close to 2% of the final value of the step change. From Tables 3.2 and 3.3 we can infer that the acceleration and jerk maximums will be inside our limit for smaller step changes, however the time required to reach the applied step within 2% will be the same for any magnitude. This leads back to the question of responsiveness. If we wish to maintain the acceleration and the jerk within the limits at the maximum step magnitude, we sacrifice responsiveness when using an RC filter.

3.2.2 A Dynamic Solution

It is possible to achieve more acceptable solutions for acceleration and jerk limitation while maintaining almost the maximum possible responsiveness. The trade-off

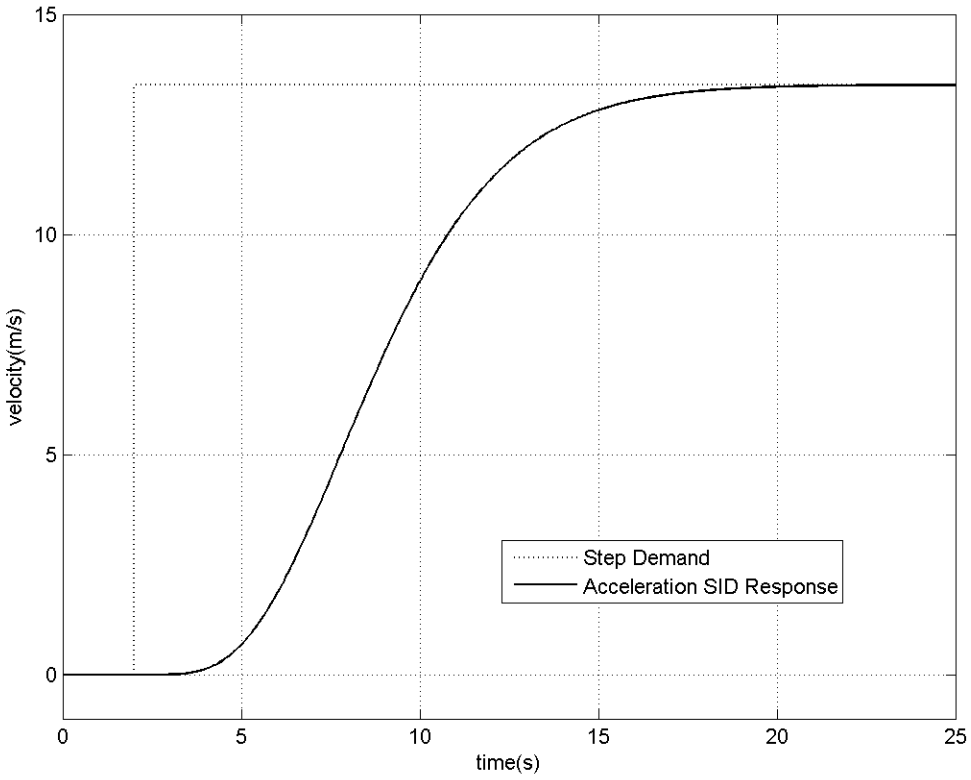

Fig. 3.4. The plant response for a $13.4\frac{\mathrm{m}}{\mathrm{s}}$ step demand using a filter with a 5-pole at $p_c = 0.75$.

for such a system is complexity. Figure 3.5 depicts a dynamic solution which limits the jerk and acceleration values effectively while giving a very good response and low delay for a variety of step magnitudes in demand. The velocity demand is applied at input one and the two limits are constant values at the left. An enable is produced by a difference between the velocity of the generated profile at output one and the velocity demand. The enable is saturated at a value of 1. A 50% attenuation is required to limit the jerk in the second half of the acceleration cycle, when the acceleration saturation limiter disengages and creates a sharp transition as deceleration occurs close to the demand magnitude. A polarity control generates positive jerk in the first half of the acceleration cycle and negative jerk in the second half of the cycle. An

integrator ($\frac{1}{s}$) then produces an acceleration curve which the acceleration saturation limiter saturates at the specified, constant limit. The dead–zone management group forces the acceleration to zero when the generated profile meets the velocity demand. The final integrator produces the generated velocity demand in Figure 3.6.

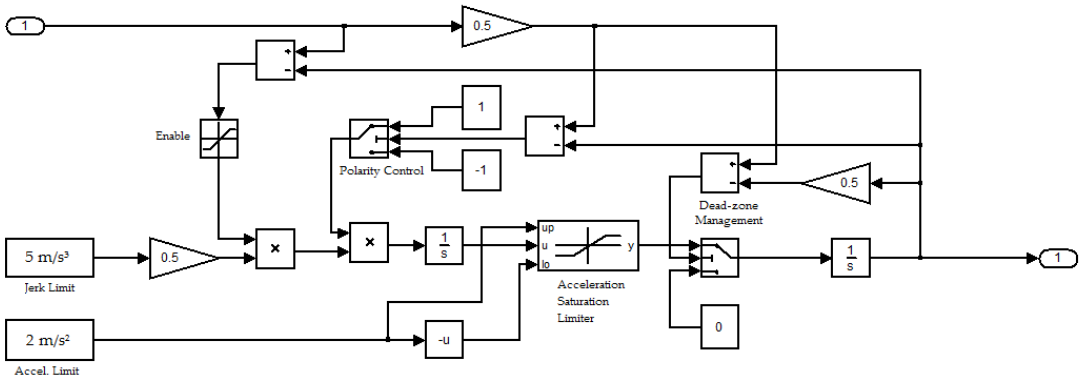

Fig. 3.5. A dynamic model which limits the acceleration and jerk in an acceleration system for a variety of step magnitudes in demand.

Using the dynamic solution to generate acceptable profiles yields the improved performance shown in Table 3.5. A comparison of this data to that determined for RC filters shows not only a great improvement for the $13.4\frac{\mathrm{m}}{\mathrm{s}}$ step magnitude, but also a response which is faster for smaller step demands and not significantly slower for larger demands. There are two values for jerk in this table that slightly exceeds the limit, for a step of $4.5\frac{\mathrm{m}}{\mathrm{s}}$ and $8.9\frac{\mathrm{m}}{\mathrm{s}}$. The maximum jerk in every case occurs near the transition to the final value. The point of maximum jerk occurs near the 10 second line, but is not obvious in the profile. Modification of the dynamic solution could provide better results in jerk limiting; particularly in regard to the corner created by the transition away from saturation limiting in the acceleration. The step demand, generated profile and acceleration system response are shown in Figure 3.6.

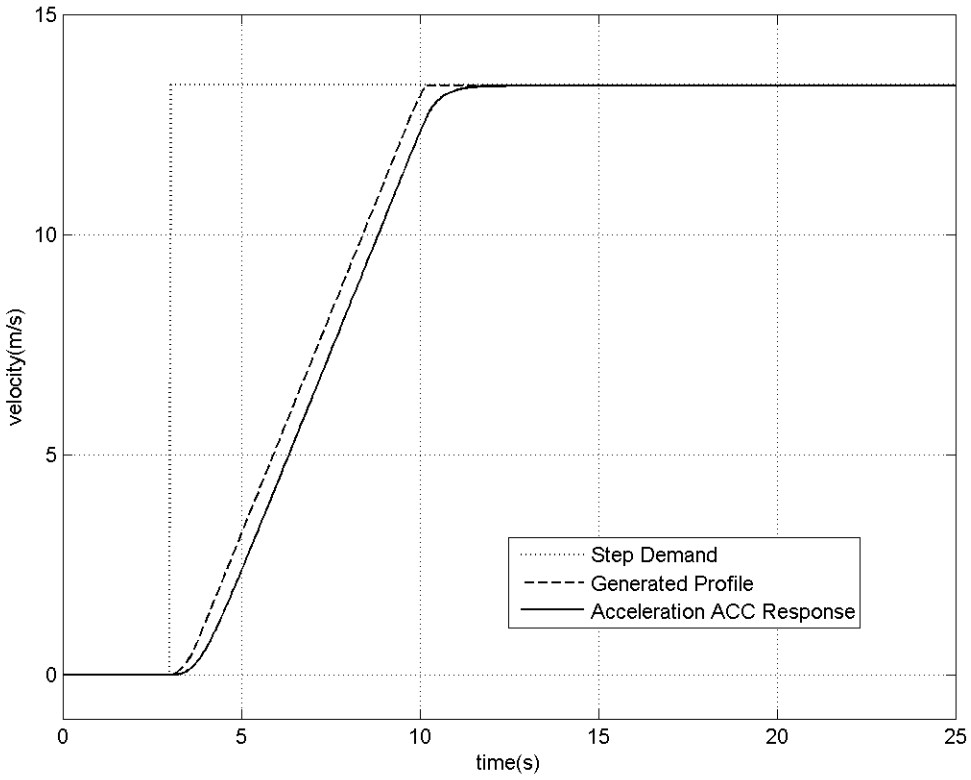

Fig. 3.6. The profile generated by a dynamic model limits both the acceleration and the jerk at very near the limits.

3.2.3 Two Hybrid Solutions

Possibly, the most desirable solution would combine aspects of the RC filter design and the dynamic design. Starting from either, we might consider the specific limitations of the design and whether something could be done to mitigate these, using the other type.

The primary limitation in the RC filter is that we sacrifice responsiveness to small demands in order to limit the acceleration and jerk in large demands. Two possible solutions are to use a rate limiter on the output of the filter to limit the acceleration or to use a switching system to change the parameters of the filter.

Table 3.5
The dynamic solution has very good metrics for a variety of step magnitudes

	Step Magnitude ($\frac{\text{m}}{\text{s}}$)				
Metric	4.5	8.9	13.4	17.9	22.4
Accel.	1.98	2.01	2.01	2.01	2.01
Jerk	5.01	5.14	4.78	4.83	4.92
Delay (s)	1.90	2.20	2.46	2.70	2.93
Response (s)	4.69	6.60	8.82	11.0	13.2

accel. in $\frac{\text{m}}{\text{s}^2}$*; jerk in* $\frac{\text{m}}{\text{s}^3}$

In the first case, an installed rate limiter is set to limit the rate of transition of the filter output to the maximum permissible acceleration. The filter may then be selected to have a faster response, reducing the delay and increasing the jerk toward the limit. Such a system is depicted in Figure 3.7 with the responses of a limited and unlimited filter in Figure 3.8. The use of a filter with multiplicity $n = 3$ and n-pole located at $p_c = 0.85$ has a response of 11 seconds. This and additional metrics of the system are described in Table 3.6.

Table 3.6
An n=3 filter with p_c=0.85 response to a 13.4$\frac{\text{m}}{\text{s}}$ step demand with and without a rate limiter.

Metric	Natural Rate	Rate-Limited
Accel.	2.66	2.00
Jerk	1.85	4.56
Delay	1.66	1.79
Response	9.33	9.34

accel. in $\frac{\text{m}}{\text{s}^2}$*; jerk in* $\frac{\text{m}}{\text{s}^3}$

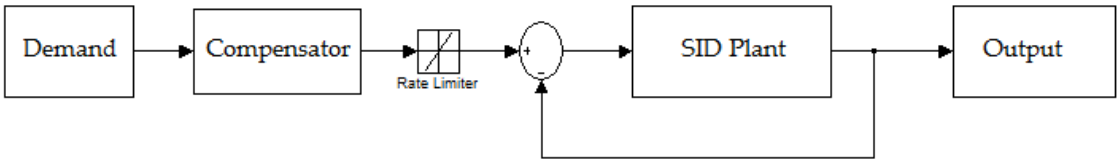

Fig. 3.7. A hybrid RC filter can be designed with a more responsive output while controlling acceleration through the use of a rate limiter.

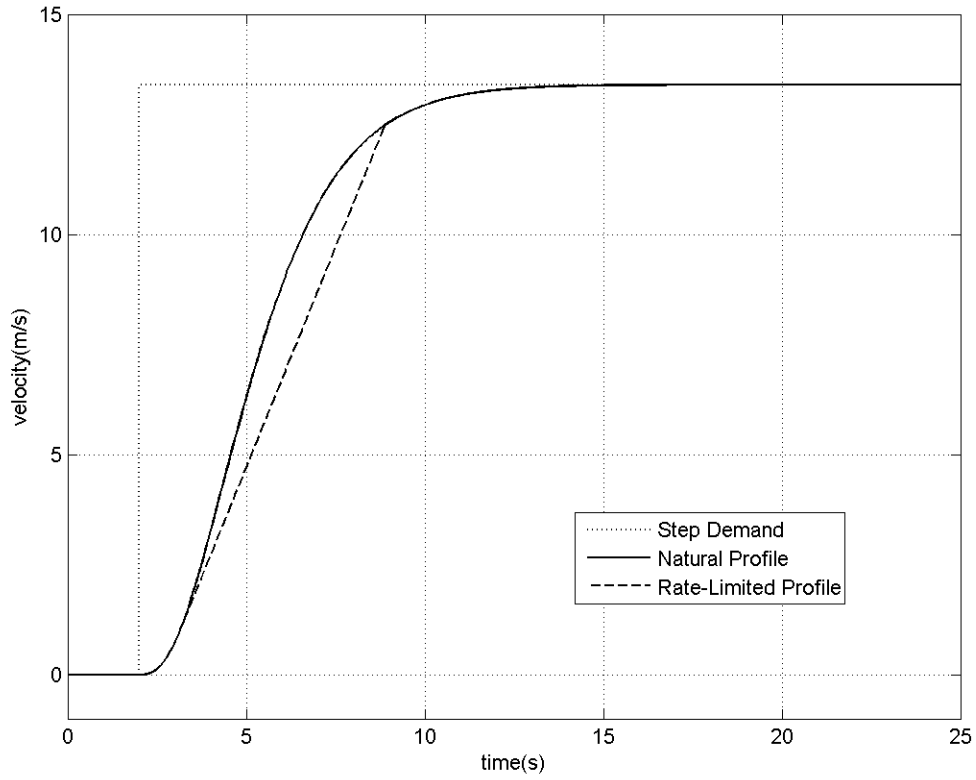

Fig. 3.8. The acceleration system response to an RC filter with and without rate limiting.

The second case of hybrid system for RC filter compensators involves switching between different RC filters based on the magnitude of the demand. Each individual

compensator might also employ rate limiting. Such a system might appear as in Figure 3.9.

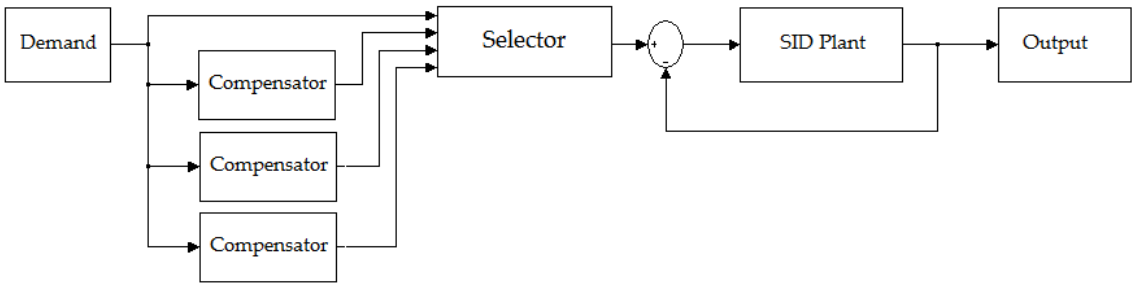

Fig. 3.9. A hybrid RC filter compensator array with individual filter compensators designed to optimize the response to various magnitudes of step demand.

3.3 Complete Profile Example

Now we investigate the response of a vehicle to the application of a realistic velocity demand. In Figure 3.10, the uncompensated vehicle responds to an applied velocity profile. The profile consists of a velocity ramp to $33.5\frac{\mathrm{m}}{\mathrm{s}}$ (75mph), followed by a decrease to $20.1\frac{\mathrm{m}}{\mathrm{s}}$ (45mph), and finally an increase to $26.8\frac{\mathrm{m}}{\mathrm{s}}$ (60mph). In response to this profile, the magnitude of the vehicle's acceleration peaks at $13.3\frac{\mathrm{m}}{\mathrm{s}^2}$ and the jerk peaks at $13.1\frac{\mathrm{m}}{\mathrm{s}^3}$. Applying the analytical jerk and acceleration limiting input filter to the acceleration and braking systems of the vehicle yields the response in Figure 3.11 for the same input profile. For this compensated system, the magnitude of acceleration peaks at $1.80\frac{\mathrm{m}}{\mathrm{s}^2}$ and the jerk peaks at $0.66\frac{\mathrm{m}}{\mathrm{s}^3}$.

3.4 Chapter Summary

The jerk of a system, $\xi = \frac{d^3x}{dt^3}$, is a measure of the smoothness of the ride, and hence the comfort. To maintain an acceptable level of comfort, the jerk should be

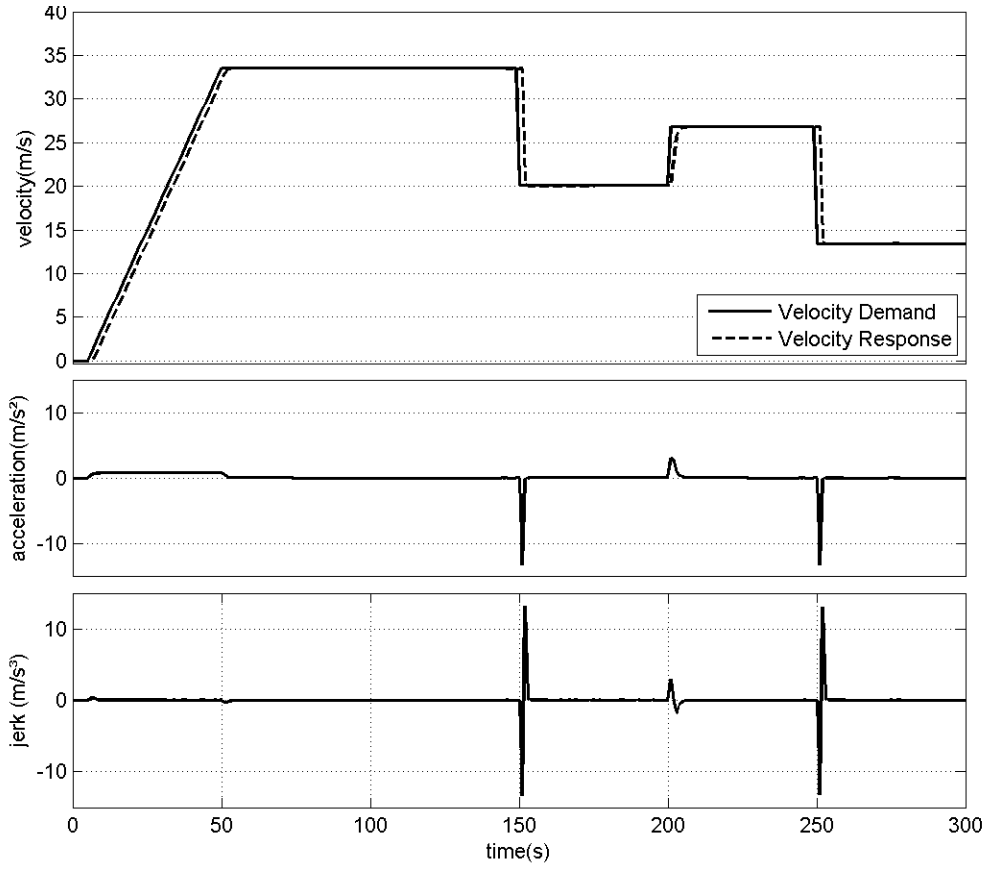

Fig. 3.10. The vehicle response to a realistic velocity demand show violations of acceleration and jerk comfort criteria.

limited in magnitude to less than $\pm 5\frac{\mathrm{m}}{\mathrm{s}^3}$, according to the University of California at Berkeley [20]. In practice, many systems which limit jerk also must limit acceleration. The University of California at Berkeley suggests $\pm 2\frac{\mathrm{m}}{\mathrm{s}^2}$ as a limit on acceleration. Jerk limit systems may range in complexity from the simple, analytical design employing passive RC filter network to a complex, active dynamic design. Both approaches have merit and both have disadvantages. A practical approach to mitigation of some of these deficiencies is to construct a hybrid system which maintains some of the simplicity of the analytical approach while gaining a measure of the faster response of the dynamic design. Finally, a realistic velocity demand profile is used to demonstrate the effectiveness of analytical jerk compensation.

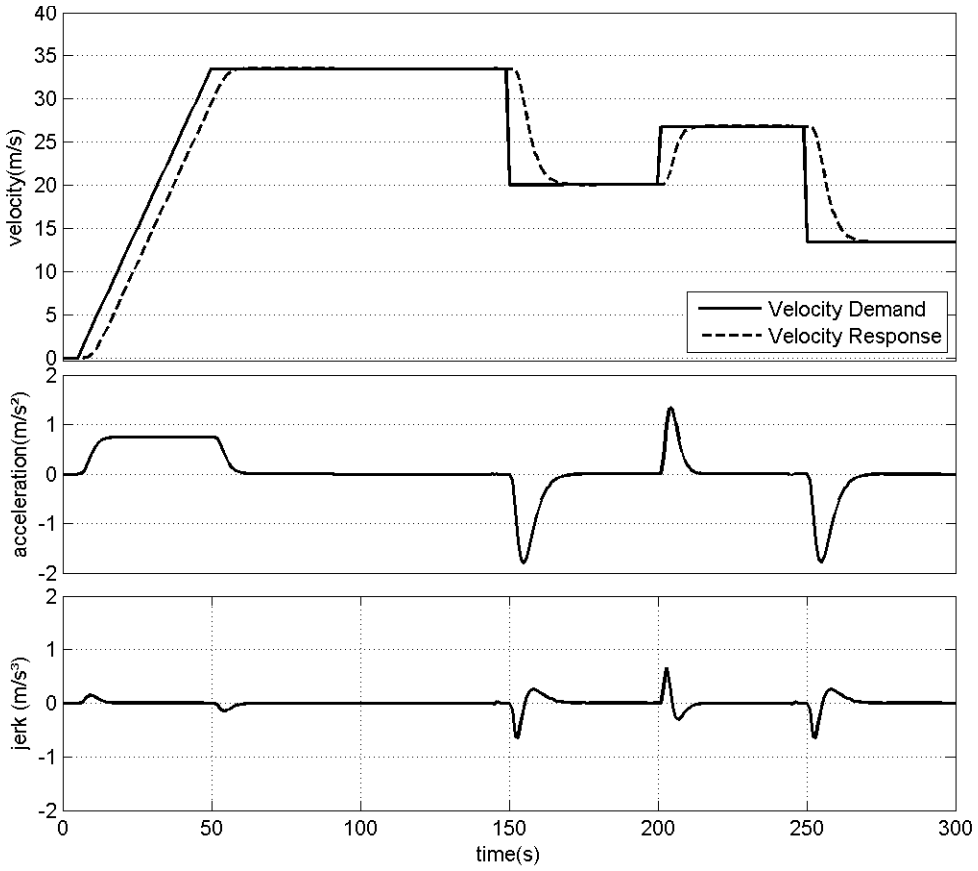

Fig. 3.11. The vehicle response to the same realistic velocity demand with analytical acceleration and jerk limiting filters for acceleration and braking systems shows acceptable results even at magnified scale.

4. PLANT ERROR COMPENSATION

In a corrupted plant, an unwanted signal called *noise* is introduced into the system. The noise may occur in various parts of the system. There may be an additive noise signal at the error signal, at the output, in the feedback loop, a gain noise in the plant, or in the feedback path. The first two types of additive noise are functionally equivalent by a factor of the transfer function of the plant. Noise may represent incidental electrical interference or a malfunction of internal components. Additionally, noise in the feedback path may be due to fluctuations in the precision of the range finding or velocity sensors of an ACC system.

4.1 Modeling a Corrupted Plant

As discussed earlier, a plant may be represented by a transfer function. In the case of this complex plant, there are two transfer functions, one for each velocity aspect of the plant. As the stability of a plant depends on the location of the poles in the complex plane, we need only be concerned with how plant corruption affects these loci [3]. It is for this reason that plant corruption can be explored as a vacillation in the coefficients of the characteristic equation of the system. These departures from the expected values may be due to noise factors or variability of sensors as mentioned, or the result of loading that occurs on the system, such as changes to wheel dynamics when snow or ice cling to them [9]. The characteristic equation is obtained by setting the denominator of the closed-loop transfer function equal to zero [3]. The closed–loop transfer function has the form: $T(s) = \frac{G(s)}{1+G(s)}$, where $G(s)$ is the open-loop transfer function. If $G(s)$ is expressed as $\frac{P(s)}{Q(s)}$, where $P(s)$ and $Q(s)$ are the numerator and denominator polynomials of $G(s)$, respectively, it follows that the characteristic equation is $Q(s) + P(s) = 0$ [3]. With the equation normalized, it

will be of the form in Equation (4.1), where the a_n are combinations of the coefficients of $P(s)$ and $Q(s)$.

$$a_n s^n + a_{n-1} s^{n-1} + a_{n-2} s^{n-2} + ... + a_0 = 0 \tag{4.1}$$

Corruption of the plant causes each of the a_n terms to fall inside some range, $\alpha_n \leq a_n \leq \beta_n$ [3]. By determining the limits of the range, we begin to shape the problem. Next, we test if the plant is stable for this range of each parameter. While it is possible to generate an infinite number of polynomials that will fit in this range, we cannot hope to solve each for its stability. Fortunately, there is a method for testing stability of any order of polynomial using only the limits of the parameter variation, and not every combination of parameter [3] [21]. For a 3rd characteristic equation, this method yields the so-called Kharitonov polynomials of (4.2) through (4.5), named after the Russian professor, Vladimir L. Kharitonov who provided the theorem [21].

$$q_1(s) = s^3 + \alpha_2 s^2 + \beta_1 s + \beta_0 \tag{4.2}$$

$$q_2(s) = s^3 + \beta_2 s^2 + \alpha_1 s + \alpha_0 \tag{4.3}$$

$$q_3(s) = s^3 + \beta_2 s^2 + \beta_1 s + \alpha_0 \tag{4.4}$$

$$q_4(s) = s^3 + \alpha_2 s^2 + \alpha_1 s + \beta_0 \tag{4.5}$$

For our transfer functions, we will initially consider a $\pm 2\%$ drift in parameters and how this affects our system. From the acceleration SID transfer function of Equation (2.20) we derive the characteristic Equation (4.6).

$$s^3 + 6.237 s^2 + 2503.7 s + 5302 = 0 \tag{4.6}$$

Now, we create a table of its coefficients and their parametric variation. Applying

Table 4.1
The parameters and the limit of their variation for a 2% uncertain acceleration system.

n	α_n	a_n	β_n
2	6.1	6.2	6.3
1	2453.6	2503.7	2553.8
0	5196	5302	5408

our acceleration system parameter ranges to Equations (4.2) through (4.5), yields the following polynomials:

$$q_1(s) = s^3 + 6.1s^2 + 2553.8s + 5408 \tag{4.7}$$

$$q_2(s) = s^3 + 6.3s^2 + 2453.6s + 5196 \tag{4.8}$$

$$q_3(s) = s^3 + 6.3s^2 + 2553.8s + 5196 \tag{4.9}$$

$$q_4(s) = s^3 + 6.1s^2 + 2453.6s + 5408 \tag{4.10}$$

Now, returning to the issue of stability—if the systems described by these polynomials are stable, then the system will be stable in the full range of variation of its parameters. We have previously discussed the root locus as a means of determining stability, now we will further examine stability as determined by the Routh–Hurwitz criterion. This test is a fast method of determining stability of a system by organizing the coefficients of the characteristic equation of the transfer function into a special form called a Routh–Hurwitz array, or RH diagram [3] [15].

The rows of the diagram are labeled with the decreasing orders of s, starting with the largest order. The arrangement of coefficients starts in the first row with the coefficient of the largest term and proceeds across with every second coefficient remaining. The second line begins with the coefficient of the second highest order and proceeds in the same fashion. The remaining rows are completed down to the s^0 row by forming a 2×2 matrix of the coefficients which occur above and just to the right

of each missing term. The missing term is assigned as the determinant of this matrix divided by the negative of the term just above the missing one. Missing terms in the 2×2 matrix are treated as zeros. The stability of the system is assured if there are no zeros or sign changes in the first column of terms in the array. Now let us construct our arrays for the acceleration system, in Table 4.2. From this collection of arrays,

Table 4.2
Routh–Hurwitz Arrays for Polynomials of Uncertain Parameters in Acceleration.

Polynomial $q_1(s)$

s^3	1	2553.8
s^2	6.1	5408
s^1	1667.2	0
s^0	5408	

Polynomial $q_2(s)$

s^3	1	2453.6
s^2	6.3	5196
s^1	1628.8	0
s^0	5196	

Polynomial $q_3(s)$

s^3	1	2553.8
s^2	6.3	5196
s^1	1729	0
s^0	5196	

Polynomial $q_4(s)$

s^3	1	2453.6
s^2	6.1	5408
s^1	1567	0
s^0	5408	

we can see that there are no sign changes or zeros. Thus the Routh–Hurwitz criteria are satisfied and our acceleration system is stable under a 2% change of parameters.

Now we will investigate the braking system. As before, we find our transfer function from Equation (2.21), and calculate our characteristic equation in (4.11). Using this, we create a table of its coefficients and their parametric variation in Table 4.1.

$$s^3 + 24.3s^2 + 2738.8s + 22894.7 = 0 \tag{4.11}$$

Table 4.3
The parameters and their variations for a 2% uncertain braking system.

n	α_n	a_n	β_n
2	23.8	24.3	24.8
1	2684.0	2738.8	2793.6
0	22436.8	22894.7	23352.6

Again, we apply the braking system parameter ranges to Equations (4.2) through (4.5) and generate four polynomials:

$$q_1(s) = s^3 + 23.8s^2 + 2793.6s + 23352.6 \tag{4.12}$$

$$q_2(s) = s^3 + 24.8s^2 + 2684.0s + 22436.8 \tag{4.13}$$

$$q_3(s) = s^3 + 24.8s^2 + 2793.6s + 22436.8 \tag{4.14}$$

$$q_4(s) = s^3 + 23.8s^2 + 2684.0s + 23352.6 \tag{4.15}$$

Finally, we apply the Routh–Hurwitz criteria as before in Table 4.4. Seeing no sign changes or zeros in the first column, we know the system is stable. Thus the Routh–Hurwitz criteria are also satisfied by our braking system, which is stable under a 2% change of parameters.

4.2 Physical Parameter Change in the Model

We have shown how changes in the coefficients of the characteristic equation may be addressed to determine stability in a system. Now let us briefly consider how changes in a physical parameter of the model may affect the characteristic equation. One physical parameter of the model which will change in regular use is the mass. We will consider a range of values in two cases, multiplicative and additive. First, consider a model instability created by a 2% margin of error in our measurement of this mass as a multiplicative error akin to the error in a sensor. For additive error,

Table 4.4
Routh–Hurwitz Arrays for Polynomials of Uncertain Parameters in Braking.

Polynomial $q_1(s)$

s^3	1	2793.6
s^2	23.8	23352.6
s^1	1812.4	0
s^0	23352.6	

Polynomial $q_2(s)$

s^3	1	2684
s^2	24.8	22436.8
s^1	1779.3	0
s^0	22436.8	

Polynomial $q_3(s)$

s^3	1	2793.6
s^2	24.8	22436.8
s^1	1888.9	0
s^0	22436.8	

Polynomial $q_4(s)$

s^3	1	2684
s^2	23.8	23352.6
s^1	1702.8	0
s^0	23352.6	

we consider a case of increased loading by adding occupants. The average mass of a human male resident of the United States is 86.6 kg [22]. The cases of the addition of one to six passengers are considered. The base mass of our model vehicle is 1500 kg. An automated process was used to generate a second order system ID model for each case and the coefficients of the characteristic equation were computed. These values and the b_{n-1} value for each characteristic equation are in Table 4.5. Table 4.6 shows the range of variation of each parameter and the percentage variation of the maximum deviation. This same process may be followed for any adjustable physical parameter of the model with similar results.

Table 4.5
The effect of physical parameter variation on the coefficients of the characteristic equation, as generated by an automated modeling program. Also, the b_{n-1} values of each.

Type	Mass(kg)	a_3	a_2	a_1	a_0	b_{n-1}
Base	1500.0	1	4.60	2687.6	6251.2	1328.7
+2%	1530.0	1	4.56	2659.0	6119.4	1317.8
-2%	1470.0	1	4.63	2717.0	6389.8	1339.8
1 Passenger	1586.6	1	4.49	2606.4	5878.3	1297.8
2 Passenger	1673.2	1	4.39	2530.3	5532.7	1269.4
3 Passenger	1759.8	1	5.06	2494.7	5295.3	1447.5
4 Passenger	1846.4	1	5.16	2448.4	5046.2	1471.1
5 Passenger	1933.0	1	5.08	2405.4	4823.8	1455.8
6 Passenger	2019.6	1	5.00	2376.6	4635.8	1449.1

Table 4.6
The range of values for variation of the coefficients of the characteristic equation due to physical parameter variation in the model.

a_n	min.	base	max.	variation(%)
a_3	1	1	1	±0
a_2	4.39	4.60	5.16	+12.24/-4.62
a_1	2376.6	2687.6	2717.0	+1.09/-11.57
a_0	4635.8	6251.2	6389.8	+2.22/-25.84

4.3 Stability Limits on Plant Corruption Through Parameter Drift

Based on these stabilities, even in the face of plant corruption, we should investigate the range of stability of our plant. To accomplish this, we first revisit our parameters from Tables 4.1 and 4.1, and replace our αs with an unknown factor γ

times a_n, and replace our βs with some λ times a_n. Both are defined in the ranges of (4.16) and (4.17).

$$0 < \gamma \leq 1 \tag{4.16}$$

$$1 \leq \lambda < \infty \tag{4.17}$$

$$\alpha_n = \gamma \cdot a_n \tag{4.18}$$

$$\beta_n = \lambda \cdot a_n \tag{4.19}$$

Table 4.7
The parameters and their variations for a variably uncertain system.

n	α_n	a_n	β_n
2	$\gamma \cdot a_2$	a_2	$\lambda \cdot a_2$
1	$\gamma \cdot a_1$	a_1	$\lambda \cdot a_1$
0	$\gamma \cdot a_0$	a_0	$\lambda \cdot a_0$

It should be clear by inspection of Tables 4.2 and 4.4 that the only term which might affect stability in this system is the first term of the s^1 row, as that is the only term which is calculated. This term, called the b_{n-1} term is defined for a 3^{rd} order system in Equation (4.20) [3].

$$b_{n-1} = \frac{1}{-a_2} \begin{vmatrix} a_3 & a_1 \\ a_2 & a_0 \end{vmatrix} = \frac{a_0 \cdot a_3 - a_1 \cdot a_2}{-a_2} \tag{4.20}$$

The condition that will cause instability in the system is when a sign change or zero occurs in the first column, and thus our condition for stability is $b_{n-1} \geq 0$. We can look at the general case as in Table 4.7 and see if simplification exists. We substitute

γ terms and λ terms as appropriate in (4.20) and simplify for the b_{n-1} term of each $q_n(s)$ equation.

$$b_{n-1}(1) = \frac{1}{-\gamma \cdot a_2} \begin{vmatrix} a_3 & \lambda \cdot a_1 \\ \gamma \cdot a_2 & \lambda \cdot a_0 \end{vmatrix} = \frac{\lambda \cdot a_0 \cdot a_3 - \gamma \cdot \lambda \cdot a_1 \cdot a_2}{-\gamma \cdot a_2} \tag{4.21}$$

$$b_{n-1}(2) = \frac{1}{-\lambda \cdot a_2} \begin{vmatrix} a_3 & \gamma \cdot a_1 \\ \lambda \cdot a_2 & \gamma \cdot a_0 \end{vmatrix} = \frac{\gamma \cdot a_0 \cdot a_3 - \gamma \cdot \lambda \cdot a_1 \cdot a_2}{-\lambda \cdot a_2} \tag{4.22}$$

$$b_{n-1}(3) = \frac{1}{-\lambda \cdot a_2} \begin{vmatrix} a_3 & \lambda \cdot a_1 \\ \lambda \cdot a_2 & \gamma \cdot a_0 \end{vmatrix} = \frac{\gamma \cdot a_0 \cdot a_3 - \lambda^2 \cdot a_1 \cdot a_2}{-\lambda \cdot a_2} \tag{4.23}$$

$$b_{n-1}(4) = \frac{1}{-\gamma \cdot a_2} \begin{vmatrix} a_3 & \gamma \cdot a_1 \\ \gamma \cdot a_2 & \lambda \cdot a_0 \end{vmatrix} = \frac{\lambda \cdot a_0 \cdot a_3 - \gamma^2 \cdot a_1 \cdot a_2}{-\gamma \cdot a_2} \tag{4.24}$$

In each case, the term b_{n-1} will be positive and non-zero if and only if the first term of the numerator of each fraction is less than the second term. This guarantees that the numerator will be negative, canceling the negative in the denominator, resulting in an all positive b_{n-1}. So we can further reduce our conditions for stability.

$$\lambda \cdot a_0 \cdot a_3 < \gamma \cdot \lambda \cdot a_1 \cdot a_2 \tag{4.25}$$

$$\gamma \cdot a_0 \cdot a_3 < \gamma \cdot \lambda \cdot a_1 \cdot a_2 \tag{4.26}$$

$$\gamma \cdot a_0 \cdot a_3 < \lambda^2 \cdot a_1 \cdot a_2 \tag{4.27}$$

$$\lambda \cdot a_0 \cdot a_3 < \gamma^2 \cdot a_1 \cdot a_2 \tag{4.28}$$

It is well understood that for a system to be stable, all the coefficients of its characteristic equations must have the same sign [3]. Thus the product of any two coefficients will be strictly positive. We may therefore collect terms to simplify further.

$$\frac{1}{\gamma} < \frac{a_1 \cdot a_2}{a_0 \cdot a_3} \tag{4.29}$$

$$\frac{1}{\lambda} < \frac{a_1 \cdot a_2}{a_0 \cdot a_3} \tag{4.30}$$

$$\frac{\gamma}{\lambda^2} < \frac{a_1 \cdot a_2}{a_0 \cdot a_3} \tag{4.31}$$

$$\frac{\lambda}{\gamma^2} < \frac{a_1 \cdot a_2}{a_0 \cdot a_3} \tag{4.32}$$

Since the right side of these inequalities are the same, let us define the reciprocal of this ratio as a constant κ which is defined for each system as in (4.33).

$$\kappa = \frac{a_0 \cdot a_3}{a_1 \cdot a_2} \tag{4.33}$$

Starting with the first two equations, it is clear that we can establish a lower limit for stability on both γ and λ. Because we have defined these variables to be strictly positive, we need not be concerned with potentially changing the direction of the inequality and so we simplify to Equations (4.34) and (4.35).

$$\gamma > \kappa \tag{4.34}$$

$$\lambda > \kappa \tag{4.35}$$

This provides us with a lower limit on the range of stability. To discover the upper range, we turn our attention to the second two equations. Again, we can safely shift the variables without changing the direction of our inequalities. Doing so results in Equations (4.36) and (4.37).

$$\gamma < \frac{1}{\kappa}\lambda^2 \tag{4.36}$$

$$\lambda < \frac{1}{\kappa}\gamma^2 \tag{4.37}$$

We now have our upper limit for stability. Combining Equations (4.34) through (4.37), we can define the ranges of γ and λ more concisely, as follows in Equations (4.38) and (4.39).

$$\kappa < \gamma < \frac{1}{\kappa}\lambda^2 \tag{4.38}$$

$$\kappa < \lambda < \frac{1}{\kappa}\gamma^2 \tag{4.39}$$

4.3.1 Further Refinement of Stability Regions

A closer examination of these equations leads to an interesting set of conditional inequalities. Comparing these equations with our initial definition for γ and λ in Equations (4.16) and (4.17), we can generate the conditional inequality condition for γ in Equation (4.40).

$$\left.\begin{array}{rl} \kappa < 0 & 0 \\ 0 \leq \kappa & \kappa \\ 0 < \kappa < 1 & \sqrt{\kappa} \end{array}\right\} < \gamma \leq \left\{\begin{array}{ll} 1 & \sqrt{\kappa} \leq \lambda \\ \frac{1}{\kappa}\lambda^2 & \lambda < \sqrt{\kappa} \end{array}\right. \tag{4.40}$$

The first value on each side of the inequality is from the initial definition of γ in Equation (4.16). The second value on each side comes from the derived expression in Equation (4.38). First, let us show that $0 < \kappa < 1$. Given that we are starting with a stable system, then from the definition of b_{n-1} in Equation (4.20) it follows that $a_3 \cdot a_0 < a_1 \cdot a_2$. Considering this with the definition of κ in Equation (4.33), it should be clear that κ is always less than 1. As observed before, the product of any two coefficients of the characteristic equation will be positive, as will the ratio of product pairs, thus we know that κ must always be positive [3]. Now, consider the last value on the left. Given that λ is less than $\frac{1}{\kappa}\gamma^2$ from Equation (4.39) and that $\gamma \in (0, 1)$ from Equation (4.16), then there must exist a point where $\frac{1}{\kappa}\gamma^2 = 1$ when $\gamma = \sqrt{\kappa}$. With κ defined as a constant, smaller values of γ would yield values less than 1, yet from Equation (4.17), λ must be greater than 1. As there can exist no λ for these values of γ satisfying the requirements for stability, γ must be greater than $\sqrt{\kappa}$. Next,

consider the other two conditional values on the left, there are competing conditions. Clearly γ must be greater than the larger of κ and $\sqrt{\kappa}$. As κ is real and always less than 1, $\sqrt{\kappa}$ will always be larger than κ. Thus the left side may be reduced to only the final value, as its condition will always be satisfied and it will always be larger than the other two values.

Now, examine the right side. Again, the first value comes from the original definition and the second value from the derivation. The conditions may be derived in a similar fashion as for the final value on the left side. Consider $\frac{1}{\kappa}\lambda^2$, for values of λ greater than $\sqrt{\kappa}$, this would be larger than 1, yet from Equation (4.16), γ cannot be greater than 1, and so this condition must be valid only for $\lambda < \sqrt{\kappa}$, leaving the first value otherwise. However, we have already determined that κ is always less than 1 and from Equation (4.16), λ is at least 1, so the condition for $\frac{1}{\kappa}\lambda^2$ can never occur. Thus the right side simplifies to only the first condition.

For λ, there exist the requirement from its definition in (4.17) and from the derivation in (4.39). Knowing that κ is always less than 1, we may take the lower limit from the definition and the upper limit from the derivation.

Putting all this information together, the final ranges of γ and λ for which the system remains stable are given in Equations (4.41) and (4.42).

$$\sqrt{\kappa} < \gamma \leq 1 \tag{4.41}$$

$$1 \leq \lambda < \frac{1}{\kappa}\gamma^2 \tag{4.42}$$

Now we can apply this condition to our acceleration and braking systems to determine how the systems can be made unstable. Given the coefficients for our acceleration and braking systems from the denominators of Equations (2.20) and (2.21), we can calculate our κ and for convenience our inverse κ. These, along with the ranges for γ and λ are shown in Table 4.8. We can draw some interesting conclusions from this data. The values for γ and λ are factors to produce a low and high value for a

Table 4.8
Conditions for stability for acceleration and braking systems in the presence of uncertain parameters.

Acceleration	Braking
$\kappa_A = 0.342$	$\kappa_B = 0.344$
$\frac{1}{\kappa_A} = 2.928$	$\frac{1}{\kappa_B} = 2.907$
$0.584 < \gamma_A \leq 1$	$0.587 < \gamma_B \leq 1$
$1 \leq \lambda_A < 2.928 \cdot \gamma_A^2$	$1 \leq \lambda_B < 2.907 \cdot \gamma_B^2$

variation range in parameters for our systems. Let us construct the percent change in the parameters in Equations (4.43) and (4.44).

$$\% \text{ decrease} = \frac{\gamma \cdot a_n - a_n}{a_n} = (\gamma - 1) \tag{4.43}$$

$$\% \text{ increase} = \frac{\lambda \cdot a_n - a_n}{a_n} = (\lambda - 1) \tag{4.44}$$

Because $\gamma \cdot a_n$ is always less than a_n, the percent change is would also be negative. Since we are considering this as the decrease already, we will use the negative of the derived value, $(1 - \gamma)$ We can compute the ranges for these percent changes from Equations (4.41) and (4.42), as shown in (4.45) and (4.46).

$$0 \leq (1 - \gamma) < 1 - \sqrt{\kappa} \tag{4.45}$$

$$0 \leq (\lambda - 1) < \frac{(1 - \gamma)^2}{\kappa} - 1 \tag{4.46}$$

Next, we plot these inequalities for each system in Figures 4.1 and 4.2. Integrating the function of the limiting curve for this region, such as in Equation (4.47), we generate a measurement of the size of the total stability region. The solution for this integral depends only on κ and is shown in Equation (4.48). This might prove to

be a useful metric for comparing the relative stability of systems in the face of plant corruption.

$$\lambda_{TOT} = \int_0^{1-\sqrt{\kappa}} \frac{(1-\gamma)^2}{\kappa} - 1 \, \mathrm{d}\gamma \tag{4.47}$$

$$\lambda_{TOT} = \frac{2}{3} \cdot \sqrt{\kappa} + \frac{1}{3 \cdot \kappa} - 1 \tag{4.48}$$

For our acceleration and braking systems, we have λ_{TOT} values of 0.365 and 0.360, respectively. We can see more generally that for a smaller percentage decrease in parameter values, there is a correspondingly larger allowable percentage increase. It is also clear that the $\pm 2\%$ variation we tested earlier is inside the stability regions of both systems.

It is interesting to determine the maximum stable uniform percentage change. The uniform percentage change would lie along the $(\lambda - 1) = (1 - \gamma)$ line and the maximum would occur on the bounding parabola, $(\lambda - 1) = \frac{1}{\kappa}(1-\gamma)^2 - 1$. Simple substitution yields the quadratic formula $\gamma^2 + (\kappa - 2)\gamma + (1 - 2 \cdot \kappa) = 0$ with one solution in the range from 0 to 1 given by Equation (4.49).

$$\gamma_{MUP} = \frac{\sqrt{\kappa^2 + 8 \cdot \kappa}}{2} + \frac{\kappa}{2} + 1 \tag{4.49}$$

For our system, this would be be equivalent to $\pm 32.7\%$ for acceleration and also $\pm 32.7\%$ for braking. This value might also be used as a simple measurement of a system's plant corruption tolerance, as modeled through uncertain parameters, although it would not be as precise.

4.3.2 Analysis of System Stability Regions

Finally, we should test a value outside the range of stability. If we allow our parameters to vary between -20% and +87%, this corresponds to a γ of 0.8 and a λ of 1.87. From Table 4.8, we can see that this value for γ is safe for both models, but while our λ value of 1.87 is safe for the acceleration system ($\lambda < 2.928(0.8)^2 = 1.874$), it is not safe for the braking system ($2.907(0.8)^2 = 1.860$). As before, we construct

our α–β values in Table 4.3.2. Now, referring back to Equations (4.2) through (4.5), we construct our R–H arrays in Tables 4.10 and 4.11.

As predicted, the parameter variation is stable for the acceleration system—there are no zeros or sign changes in the first column of any of the arrays in Table 4.10. The variation was unstable for the braking system, as indicated by the sign change in first column of the R–H array of the $q_4(s)$ polynomial in Table 4.11.

4.4 Robust Control and Error Compensation

Now that we have shown the particulars of plant error modeling through uncertain parameters, we must address plant error compensation. Our objective is to apply a robust controller that will bring the plant back into stable operation. We will compensate the plant by the use of a cascade controller such as depicted in Figure 1.1. The open-loop transfer function of the compensated system is obtained as the product of the controller and plant transfer functions [3]. We begin with the acceleration open-loop SID transfer function of equation (2.20) We will assume that the real pole will remain stable under uncertain parameters. This is a reasonable assumption, based on the path of this pole in the root locus plot of Figure B.3. Our controller substitutes a pole by placing a zero at the location of the real pole while having a pole at some new

Table 4.9
The parameters and their variations for a $-20/+87\%$ uncertain acceleration and braking systems.

Acceleration				Braking			
n	α_n	a_n	β_n	n	α_n	a_n	β_n
2	5	6.2	11.6	2	19.4	24.3	45.4
1	2003	2503.7	4681.9	1	2191	2738.8	5121.6
0	4241.6	5302	9914.7	0	18315.8	22894.7	42813.1

Table 4.10
Routh–Hurwitz Arrays for Polynomials of $-20/+87\%$ Uncertain Parameters in Acceleration.

Polynomial $q_1(s)$

s^3	1	4681.9
s^2	5	9914.7
s^1	2699	0
s^0	9914.7	

Polynomial $q_2(s)$

s^3	1	2003
s^2	11.6	4241.6
s^1	1637.3	0
s^0	4241.6	

Polynomial $q_3(s)$

s^3	1	4681.9
s^2	11.6	4241.6
s^1	4316.2	0
s^0	4241.6	

Polynomial $q_4(s)$

s^3	1	2003
s^2	5	9914.7
s^1	20.1	0
s^0	9914.7	

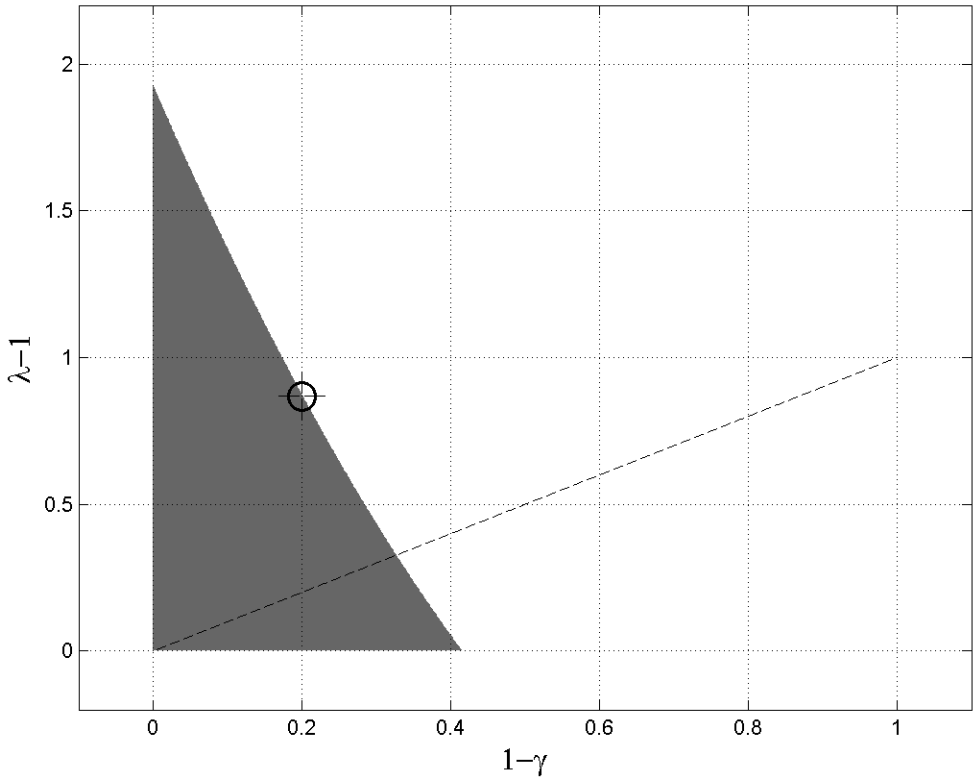

Fig. 4.1. The range of stable percent change for the SID2 acceleration system, showing the line of uniform percent change and the location of the selected test criteria.

Table 4.11
Routh–Hurwitz Arrays for Polynomials of $-20/+87\%$ Uncertain Parameters in braking.

Polynomial $q_1(s)$

s^3	1	5121.6
s^2	19.4	42813.1
s^1	2914.7	0
s^0	42813.1	

Polynomial $q_2(s)$

s^3	1	2191
s^2	45.4	18315.8
s^1	1787.6	0
s^0	18315.8	

Polynomial $q_3(s)$

s^3	1	5121.6
s^2	45.4	18315.8
s^1	4718.2	0
s^0	18315.8	

Polynomial $q_4(s)$

s^3	1	2191
s^2	19.4	42813.1
s^1	**-15.9**	0
s^0	42813.1	

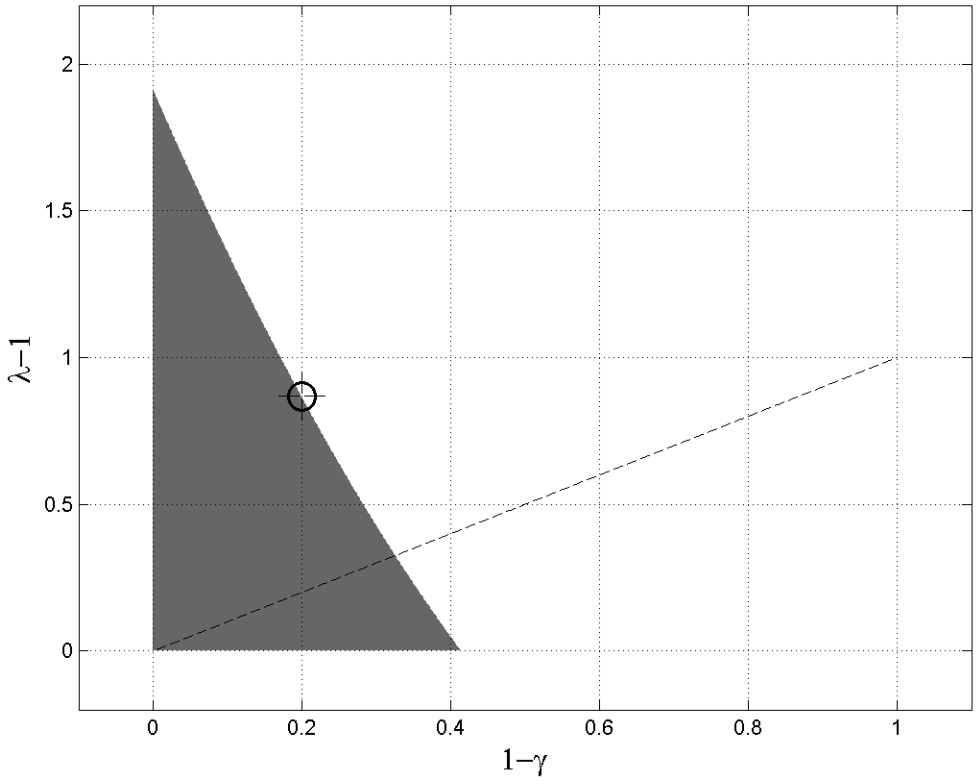

Fig. 4.2. The range of stable percent change for the SID2 braking system, showing the line of uniform percent change and the location of the selected test criteria.

location. It would likely be possible to find a solution for the compensator using only one pole; however, we will use this method to maintain our characteristic equation at third order, both to minimize complexity and to allow an easy comparison with work in this chapter. The transfer function of our compensator begins to take shape in Equation (4.50).

$$G_c(s) = K_c \cdot \frac{(s + z_c)}{(s + p_c)} \tag{4.50}$$

Next, we multiply these two equations together, setting $z_c = 1.157$ to cancel the common factor, and arrive at the compensated open-loop Equation (4.51).

$$G_c(s)G(s) = \frac{1.383 \cdot K_c \cdot (s + 1803)}{s^3 + (p_c + 5.08)s^2 + (5.08 \cdot p_c + 2496.5)s + (2496.5 \cdot p_c)} \tag{4.51}$$

Now, the closed-loop characteristic equation is constructed in the usual way in Equation (4.52). The coefficients of this equation are then given uniform uncertainty in Table 4.12.

$$s^3 + (p_c + 5.08)s^2 + (5.08 \cdot p_c + 2496.5 + 1.383 \cdot K_c)s + (2496.5 \cdot p_c + 1803 \cdot K_c) = 0 \tag{4.52}$$

It can be verified by inspection of Figure 4.1 that the acceleration system is unstable for a uniform parameter drift of 40%. The method of analysis has been shown previously. Repeating the process for this value of uncertainty shows that the instability occurs in the R–H array of $q_4(s)$ in Table 4.13. Compensation can be achieved by selecting stable values for K_c and p_c. This can be accomplished numerically or analytically.

4.4.1 A Numerical Solution

It is possible to investigate our pole location and gain by means of a computer program, analogous to plotting the $2n$–b–ω space in Chapter 3. Such a program as appears in Appendix C generates the surface in Figure 4.3 for our system. Using such a program, we might choose $K_c = 1$ and $p_c = 0.5$ as stable values to compensate our

Table 4.12
The parameters of the compensated acceleration system are perturbed as before.

n	α_n	a_n	β_n
2	$\gamma \cdot (p_c + 5.08)$	$(p_c + 5.08)$	$\lambda \cdot (p_c + 5.08)$
1	$\gamma \cdot (5.08 \cdot p_c + 2496.5 + 1.383 \cdot K_c)$	$(5.08 \cdot p_c + 2496.5 + 1.383 \cdot K_c)$	$\lambda \cdot (5.08 \cdot p_c + 2496.5 + 1.383 \cdot K_c)$
0	$\gamma \cdot (2496.5 \cdot p_c + 1803 \cdot K_c)$	$(2496.5 \cdot p_c + 1803 \cdot K_c)$	$\lambda \cdot (2496.5 \cdot p_c + 1803 \cdot K_c)$

Table 4.13
Routh–Hurwitz Arrays for Polynomials of ±40% uncertain parameters in acceleration.

Polynomial $q_1(s)$

s^3	1	3505.2
s^2	2.5	7422.8
s^1	536.1	0
s^0	7422.8	

Polynomial $q_2(s)$

s^3	1	1001.5
s^2	8.7	2120.8
s^1	757.7	0
s^0	2120.8	

Polynomial $q_3(s)$

s^3	1	3505.2
s^2	8.7	2120.8
s^1	3261.4	0
s^0	2120.8	

Polynomial $q_4(s)$

s^3	1	1001.5
s^2	2.5	7422.8
s^1	**-1967.6**	0
s^0	7422.8	

our system. The resulting characteristic equation with these values from Equation (4.52) is (4.53).

$$s^3 + 5.58 \cdot s^2 + 2500 \cdot s + 3051 = 0 \tag{4.53}$$

By plotting the R–H array for these values in Table 4.14, we see the system has been brought back into stability.

4.4.2 An Analytical Solution

For our compensator design, we examine the $q_4(s)$ R–H array with our compensation pole in place in Table 4.15. As in the derivations above, we look more closely at b_{n-1}, which is the only location where a sign change may occur in the first column. This term is defined in Equation (4.54).

$$\left(\gamma \cdot (5.08 \cdot p_c + 2496.5 + 1.383 \cdot K_c) - \frac{\lambda \cdot (2496.5 \cdot p_c + 1803 \cdot K_c)}{\gamma \cdot (p_c + 5.08)}\right) \tag{4.54}$$

We want to solve the conditions for stability on p_c. The second term denominator yields $p_c \neq -5.08$, however stability dictates that all poles fall in the left half s-plane, thus $p_c > 0$, which includes the earlier requirement. We may approach the solution by defining the boundary conditions for stability. $b_{n-1} = 0$ forms one boundary condition. $p_c > 0$ and $K_c > 0$ will form the other boundary conditions. Setting $b_{n-1} = 0$ from Table 4.15 and solving for K_c yields Equation (4.55).

$$K_c = \frac{-2983.5 \cdot \lambda \cdot p_c - 2353330.6 \cdot \lambda}{\gamma^2 \cdot (p_c + 5.08) - 1303.7 \cdot \lambda} - 3.673 \cdot p_c - 1805.1 \tag{4.55}$$

At this point, we apply $\gamma = 1 - 0.4 = 0.6$ and $\lambda = 1 + 0.4 = 1.4$ to Equation (4.55) and simplify to Equation (4.56).

$$K_c = \frac{-67917123.3}{p_c - 5064.8} - 3.673 \cdot p_c - 13407.8 \tag{4.56}$$

When plotted, the relationship is very linear near the origin, as in Figure 4.4. Solving for $K_c = 0$ and then for $p_c = 0$, we can calculate the linear relationship near the origin as Equation (4.57).

$$K_c = 1.025 \cdot p_c + 1.811 \tag{4.57}$$

Table 4.14
Routh–Hurwitz Arrays for Polynomials of ±40% uncertain parameters in compensated acceleration.

Polynomial $q_1(s)$

s^3	1	3500
s^2	3.3	4271.4
s^1	2205.6	0
s^0	4271.4	

Polynomial $q_2(s)$

s^3	1	1500
s^2	7.8	1830.6
s^1	1265.3	0
s^0	1830.6	

Polynomial $q_3(s)$

s^3	1	3500
s^2	7.8	1830.6
s^1	3265.3	0
s^0	1830.6	

Polynomial $q_4(s)$

s^3	1	1500
s^2	3.3	4271.4
s^1	205.6	0
s^0	4271.4	

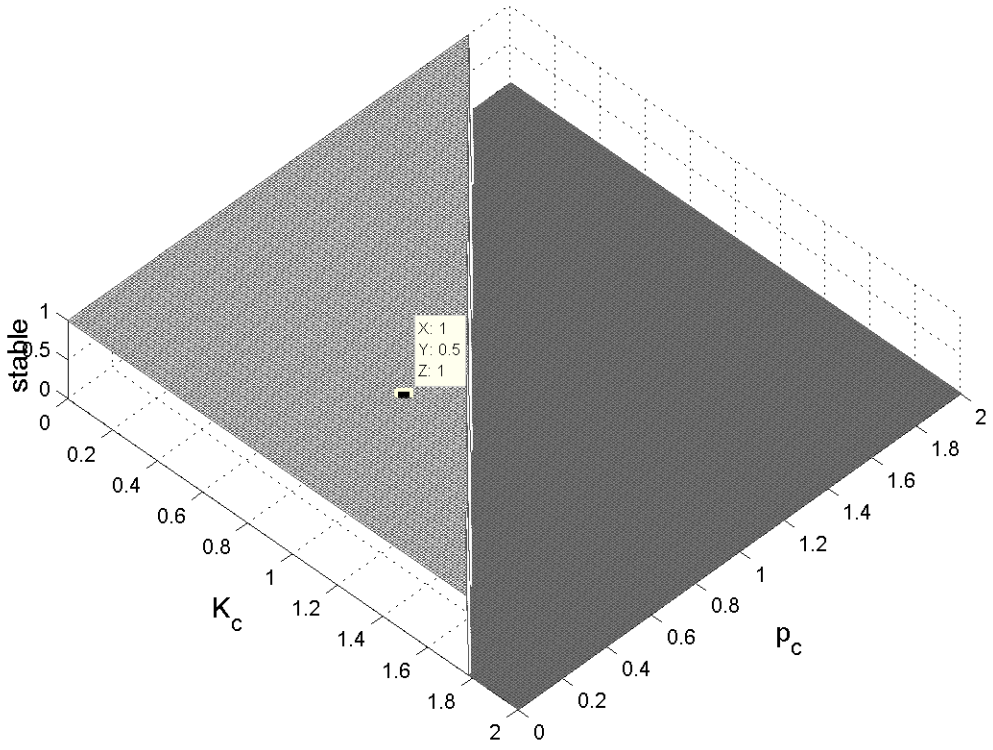

Fig. 4.3. The stable values of p_c and K_c for our 40% uniform uncertainty, highlighting a combination which will yield stability in our system.

Table 4.15
The compensated acceleration system's $q_4(s)$ equation with an unknown compensator root and gain.

$q_4(s)$ RH Array Calculation

s^3	1	$\gamma \cdot (5.08 \cdot p_c + 2496.5 + 1.383 \cdot K_c)$
s^2	$\gamma \cdot (p_c + 5.08)$	$\lambda \cdot (2496.5 \cdot p_c + 1803 \cdot K_c)$
s^1	$\left(\gamma \cdot (5.08 \cdot p_c + 2496.5 + 1.383 \cdot K_c) - \frac{\lambda \cdot (2496.5 \cdot p_c + 1803 \cdot K_c)}{\gamma \cdot (p_c + 5.08)}\right)$	0
s^0	$\lambda \cdot (2496.5 \cdot p_c + 1803 \cdot K_c)$	

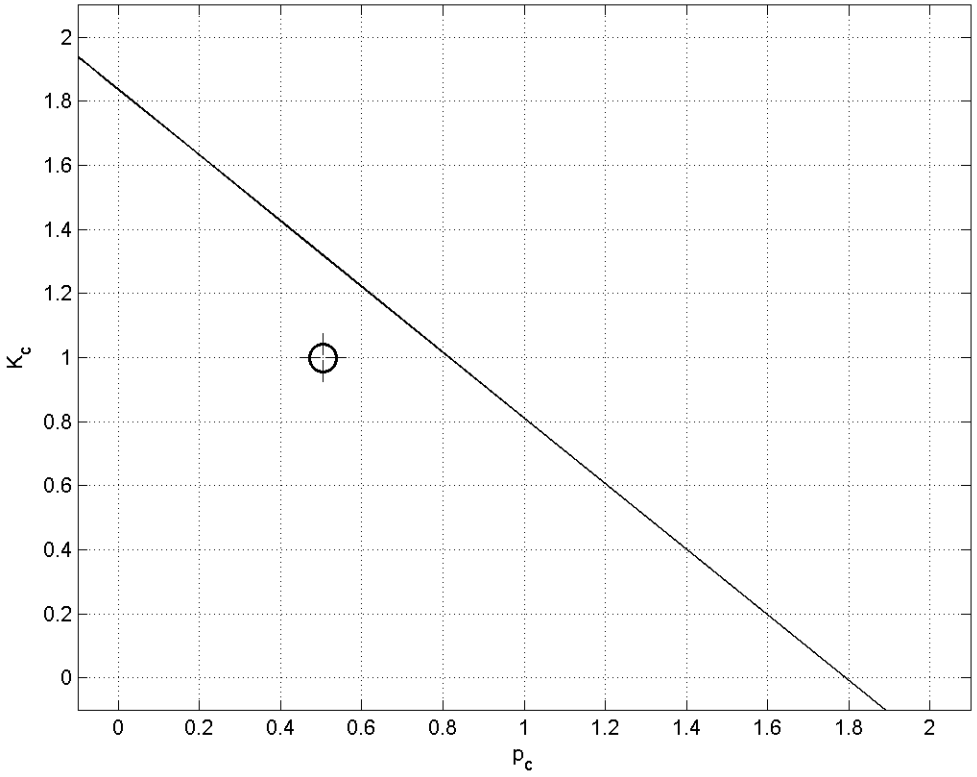

Fig. 4.4. The boundary relationship between p_c and K_c for 40% uniform uncertainty with the gain–pole location of (1,0.5) marked.

This condition forms a triangular region of stability as predicted by our numerical solution. For completeness, we must check that this boundary is an upper limit. Returning to Equation (4.55), we substitute a point below the line of Equation (4.57). Choosing $(K_c, p_c) = (0, 0)$ and requiring a positive value simplifies to yield the condition of γ and λ in (4.58).

$$\frac{1}{1 - 256.6 \cdot \frac{\lambda}{\gamma^2}} < 0 \tag{4.58}$$

This condition is satisfied for all values of γ and λ in the limits already established, therefore the boundary of (4.57) is an upper limit. Finally, our limits on K_c and p_c may be collected as in Equations (4.59) and (4.60).

$$0 < K_c < 1.025 \cdot p_c + 1.811 \tag{4.59}$$

$$0 < p_c < 0.976 \cdot K_c - 1.767 \tag{4.60}$$

Once again, choosing $K_c = 1$ and $p_c = 0.5$ will satisfy these conditions.

Our completed compensator design is Equation (4.61) and the compensated open-loop transfer function of our system is Equation (4.62).

$$G_c(s) = \frac{(s + 1.157)}{(s + 0.5)} \tag{4.61}$$

$$G_c(s)G(s) = \frac{s + 1803}{s^3 + 5.508 \cdot s^2 + 2499 \cdot s + 1248} \tag{4.62}$$

4.5 Chapter Summary

In this chapter, we have explored the stability of our vehicle model in the face of plant corruption. We have discussed the modeling of a corrupted plant using a technique of uncertain parameters. Finding that the plant is stable under a proposed 2% change in parameters, we investigated what would be required to cause instability in the plant. A procedure for determining the range of stable parameter variation has been introduced in Equations (4.41) and (4.42). The procedure was then applied to the system ID models of the acceleration and braking systems, and stable and unstable cases were explored. Two possible metrics for rating the parameter uncertainty tolerance have been suggested. The first relates to the total area of the γ–λ stability region and is defined in Equation (4.48). The second relates to the magnitude of maximum uniform stable parameter variation, as determined by solving the single Equation (4.49).

Finally, we addressed the issue of plant error compensation. A method of compensation was explored and applied to a corrupted acceleration model. The compensator

design substitutes a pole in the open-loop transfer function, allowing selection of a new pole to bring the system back into stable operation. The stable location of this pole depends on the magnitude of uniform uncertainty and on the compensator gain, K_c. Careful selection of this gain allows us to bring the errant plant back into stability. A numerical solution was demonstrated using a short MatLAB program to determine the range of possible locations of p_c and values of K_c yielding stable operation. Finally, an analytical analysis of the pole location was presented. The analytical solution showed that boundary conditions for the stability region may be derived from the R–H array and this solution agreed with the numerical approach.

5. SUMMARY

In Chapter 1, we have discussed a fundamental understanding of what comprises a controlled system. We have explained the broad operational parameters of an adaptive cruise control system and listed the primary disturbances to such a system in Table 1.2. We discussed previous work in the field by Yao Zhai. We also discussed the nature of our dynamic model and introduced the three primary topics of discussion for this thesis: System Identification, Jerk Compensation, and Plant Error Compensation.

Moving on to Chapter 2, we explored the method of system identification further and applied the process to a part of the problem at hand. The successful creation of a system ID model depends on proper determination of time constants and gain. By employing a manual curve-fitting technique, the appropriate system identification model for acceleration was derived from step response data. This model was used in subsequent chapters for analysis and compensation of the jerk in Chapter 3. We also used the transfer function for this system identity to explore plant corruption through the method of uncertain parameters in Chapter 4.

In Chapter 3, we discussed limiting the jerk of an adaptive cruise control system to enhance the comfort of the passengers. To maintain an acceptable level of comfort, the jerk should be limited in magnitude to less than 11.2 $\frac{\text{mph}}{\text{s}^2}$, according to the University of California at Berkeley. Systems which limit jerk also must limit acceleration. The University of California at Berkeley suggests 4.5 $\frac{\text{mph}}{\text{s}}$ as a limit on acceleration. Jerk limit systems may range in complexity from the simple, analytical design, employing a passive RC filter network, to a complex, active dynamic design. We have demonstrated designs of both types which successfully limit the jerk of an ACC system under normal operating parameters. Both designs have merit and both have deficiencies. Two hybrid designs were discussed which capitalize on beneficial

aspects of each type of system. Such a design is a practical approach to mitigation of some of the deficiencies of each type of system. A realistic velocity profile was demonstrated with and without jerk compensation.

Finally, in Chapter 4, we explored the stability of our vehicle model to plant corruption. We discussed the modeling of a corrupted plant using a technique of uncertain parameters. We applied this technique to create a minor corruption of 2% and used analytical techniques to investigate. We also explored how variations of model parameters effected variations in the characteristic equation. Finding that both acceleration and braking models were stable, we performed further analysis on what would be required to cause instability in the plants. A procedure for determining the range of stable parameter variation was introduced in Equations (4.41) and (4.42). The procedure was applied to the system ID models of the acceleration and braking systems, and stable and unstable cases were explored. Two possible metrics for rating the parameter uncertainty tolerance have been suggested. The first relates to the total area of the γ–λ stability region and is defined in Equation (4.48). The second relates to the magnitude of maximum uniform stable parameter variation, as determined by solving the single intersection of curves, yielding Equation (4.49).

Finally, we addressed the issue of plant error compensation. A method of compensation was explored and applied to a corrupted acceleration model. The compensator design substitutes a pole in the open-loop transfer function, allowing selection of a new pole to bring the system back into stable operation. The stable location of this pole depends on the magnitude of uniform uncertainty and on the compensator gain, K_c. Careful selection of this gain allows definition of a region of stability for the compensator pole. A numerical solution for the selection of pole location and gain was demonstrated as was an analytical solution.

5.1 Conclusions

Employing system identification is a viable means of reducing the complexity of a problem. Indeed, in some cases, the only way to state the problem accurately would be the generation of a model to fit a set of data, such as by using system identification. Once such a model is obtained, the application of analytical techniques can yield practical results quickly.

Jerk limitation in adaptive cruise control systems is achieved in the same fashion as it would be in any other situation. The practicality of applying a jerk control system to an ACC system is in the ability to define the step changes which may occur regularly in such a system. The fact that these changes are limited in magnitude compared to the full range possible in an automobile increases the likelihood for the existence of a practical solution.

Plant error is likely to occur in any implemented system. The importance of the ability to analyze and compensate for the error cannot be understated. For a given system, a quick analysis of the range of stability to a uniform parameter uncertainty is a practical, and easily-applied metric in the comparison of competing designs. For a system which is known to be unstable via the methods of uncertain parameters, compensation can be achieved through placing an additional pole and solving for the range of stable values.

LaTeX is an excellent resource for the production of professional documents. It provides a particularly great environment for the presentation of formulae. The LaTeX Companion is a great resource for formatting questions [23].

5.2 Further Work

Continued research in jerk limitation could be focused along several avenues of discussion. First, a researcher might be tempted to investigate the use of additional filter architectures, such as Salen-Key for Chebyshev or Butterworth filters. Second, an investigation of improved methods of generating a profile based on a step demand

in the dynamic design could be investigated. Specifically, a better method of merging both the acceleration limit and the jerk limit in real time. Finally, a more detailed analysis of the hybrid designs could be considered.

In the field of plant error, there are a number of opportunities for research. The applicability of a γ–λ process to higher order systems is worth investigating, particularly if it might yield a generalized form to calculate the stability regions of a plant of arbitrary degree with uncertain parameters. For a second or third order system, investigating the effect of a non–uniform uncertainly profile, and how this affects the proposed stability measures is warranted.

LIST OF REFERENCES

LIST OF REFERENCES

[1] Y. Zhai, "Design of switching strategy for adaptive cruise control under string stability constraints," Master's thesis, Purdue University, 2010.

[2] P. Horowitz and W. Hill, *The Art of Electronics*. Cambridge, United Kingdom: Cambridge University Press, second ed., 1989.

[3] R. C. Dorf and R. H. Bishop, *Modern Control Systems*. Upper Saddle River, New Jersey: Pearson Education Inc., twelth ed., 2011.

[4] "Preview distance control," online, Highway Industry Development Organization, November 2000. *http://www.hido.or.jp/ITSHP_e/wi/itshb/Preview.htm*.

[5] "Volvo s60 features and options," online, Volvo Cars, retrieved February 2012. *http://www.volvocars.com/us/all-cars/volvo-s60/details*.

[6] "Build your own 2012 750li xdrive sedan," online, BMW USA, retrieved February 2012. *http://www.bmwusa.com/Standard/Content/BYO*.

[7] "2013 taurus—adaptive cruise control technology," online, Ford Motor Company, retrieved February 2012. *http://www.ford.com/cars/taurus/features/#page=Feature19*.

[8] U. Kiencke and L. Nielsen, *Automotive Control Systems*. Berlin Heidelberg, Germany: Springer-Verlag, second ed., 2010.

[9] J.-J. E. Slotine and W. Li, *Applied Nonlinear Control*. Englewood Cliffs, New Jersey: Prentice-Hall, Inc., 1991.

[10] "Faculty areas of interest," online, Transportation Active Safety Institute, retrieved February 2012. *http://www.tasi.iupui.edu/interest*.

[11] J. Clarkson, R. Hammond, and J. May, "Episode #18.5," tech. rep., Top Gear, February 2012. British Broadcasting Corporation (BBC), UK.

[12] C.-T. Chen, *Linear System Theory and Design*. New York, New York: Oxford University Press, third ed., 1999.

[13] M. L. Boas, *Mathematical Methods in the Physical Sciences*. New York, New York: John Wiley & Sons, Inc., second ed., 1983.

[14] B. P. Lathi, *Linear Systems and Signals*. New York, New York: Oxford University Press, second ed., 2005.

[15] S. H. Żak, *Systems and Control*. New York, New York: Oxford University Press, 2003.

[16] E. J. Mastascusa, "System identification using time domain data," online, Bucknell University, December 2009. *http://www.facstaff.bucknell.edu/mastascu/econtrolhtml/Ident/Ident1.htm*.

[17] R. C. Gonzalez and R. E. Woods, *Digital Image Processing*. Englewood Cliffs, New Jersey: Prentice Hall, second ed., 2002.

[18] B. Y. Creer, U. Harald A Smedal, Cpt., and R. C. Wingrove, "Centrifuge study of pilot tolerance to acceleration and the effects of acceleration on pilot performance," tech. rep., Ames Research Cetner, Moffett Field, California, November 1960.

[19] P. Zitzewitz, *Merrill Physics Principles and Problems*. New York: Glencoe, 1995.

[20] J. Frankel, L. Alvarez, R. Horowitz, and P. Li, "Robust platoon maneuvers for avhs," tech. rep., Institute of Transportation Studies, University of California, Berkeley, November 1994.

[21] W. J. Grantham and T. L. Vincent, *Modern Control Systems Analysis and Design*. New York, New York: John Wiley & Sons, Inc., 1993.

[22] P. Cynthia L. Ogden, M. Cheryl D. Fryar, M. Margaret D. Carroll, and P. Katherine M. Flegal, "Mean body weight, height, and body mass index, united states 1960-2002," Advance data from vital and health statistics 347, U.S. Department of Heath and Human Services, Hyattsville, Maryland: National Center for Heath Statistics, October 2004.

[23] M. Goossens, F. Mittelbach, and A. Samarin, *The LaTeX Companion*. Reading Massachusetts: Addison-Wesley, 1994.

APPENDICES

A. Additional Data

The following pages contain additional or supplementary data. Figure A.2 shows the unfiltered data for the 2n–b–ω space defined in Chapter 2. Figure A.3 has the same data after being recursively filtered by the 3×3 gaussian filter as in Equation (A.1). This operation smooths the data by reducing the variation between adjacent points. The data was then trimmed, as filtering n-times produces a margin of noise of n points on each side of the data set.

$$H(s) = \begin{vmatrix} 0.0113 & 0.0838 & 0.0113 \\ 0.0838 & 0.6193 & 0.0838 \\ 0.0113 & 0.0838 & 0.0113 \end{vmatrix} \tag{A.1}$$

Figure A.4 depicts a more dramatic example of a $10\times$ gaussian–filtered 2n–b–ω space with the original data inset. This data was generated by the author for a second order system ID similar to that used for the acceleration system.

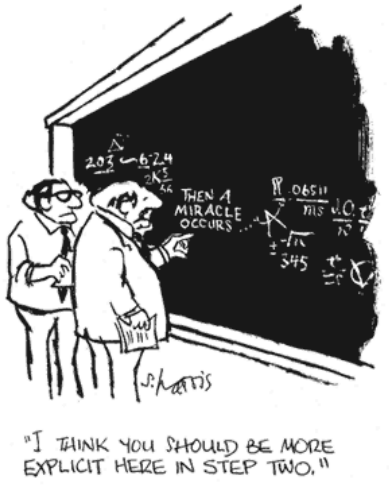

Fig. A.1. Copyright 2006 by Sidney Harris.

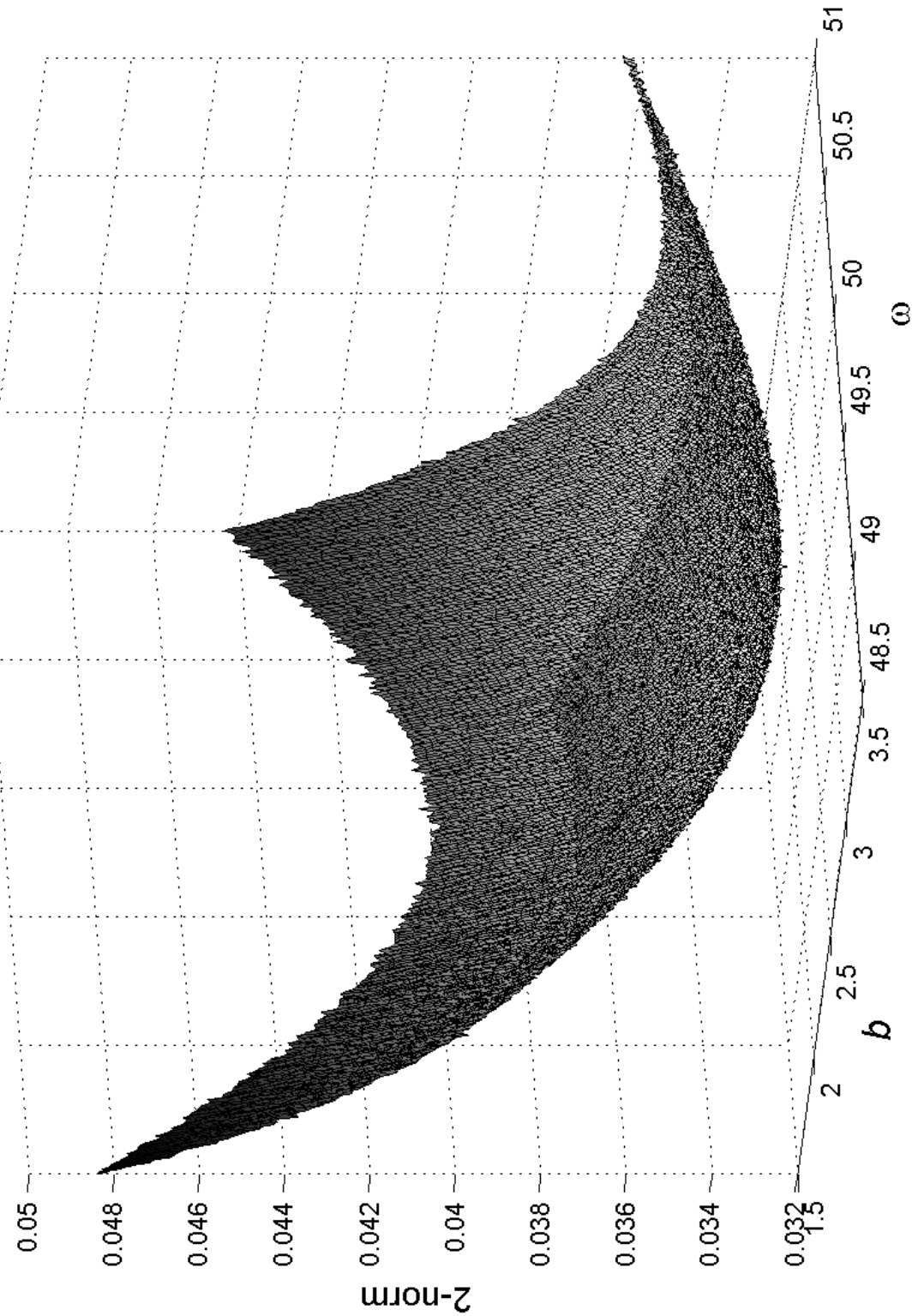

Fig. A.2. Raw data for the 2n–b–ω space discussed in Chapter 2, showing unfiltered noise.

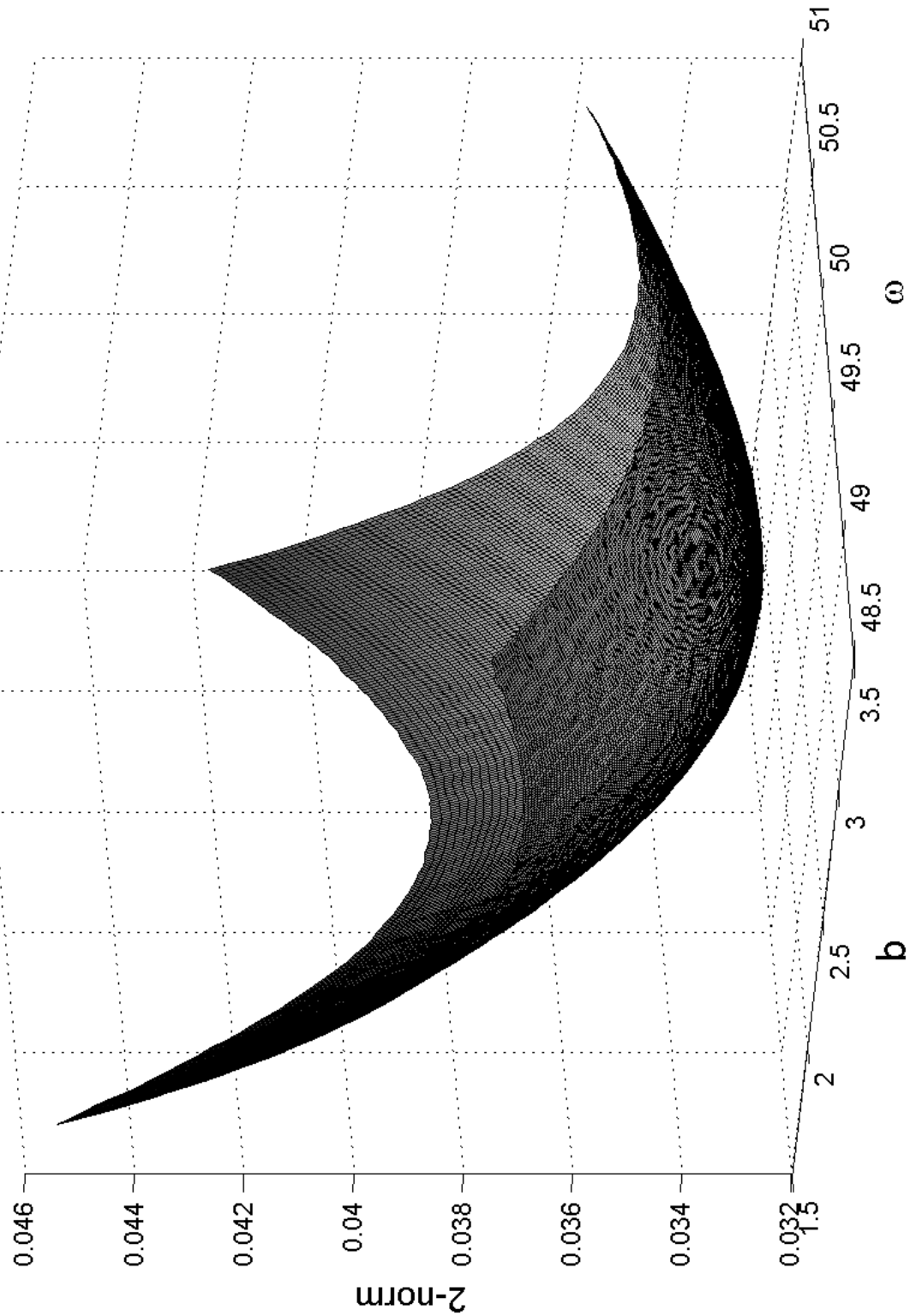

Fig. A.3. 10x gaussian filtered data for the 2n–b–ω space discussed in Chapter 2.

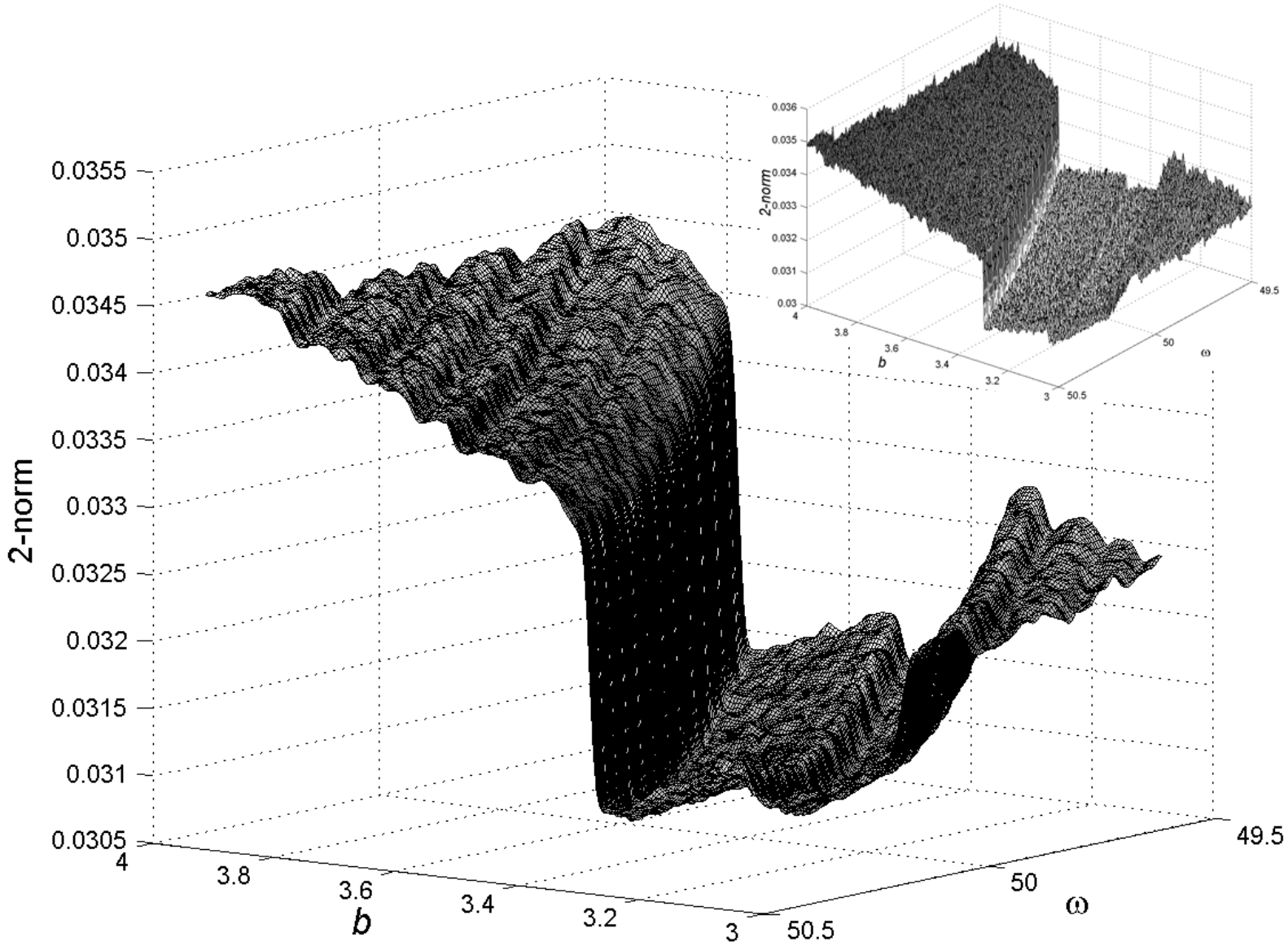

Fig. A.4. 10x gaussian filtered data for an additional, more complex 2n–b–ω space.

B. System ID Analysis Plots

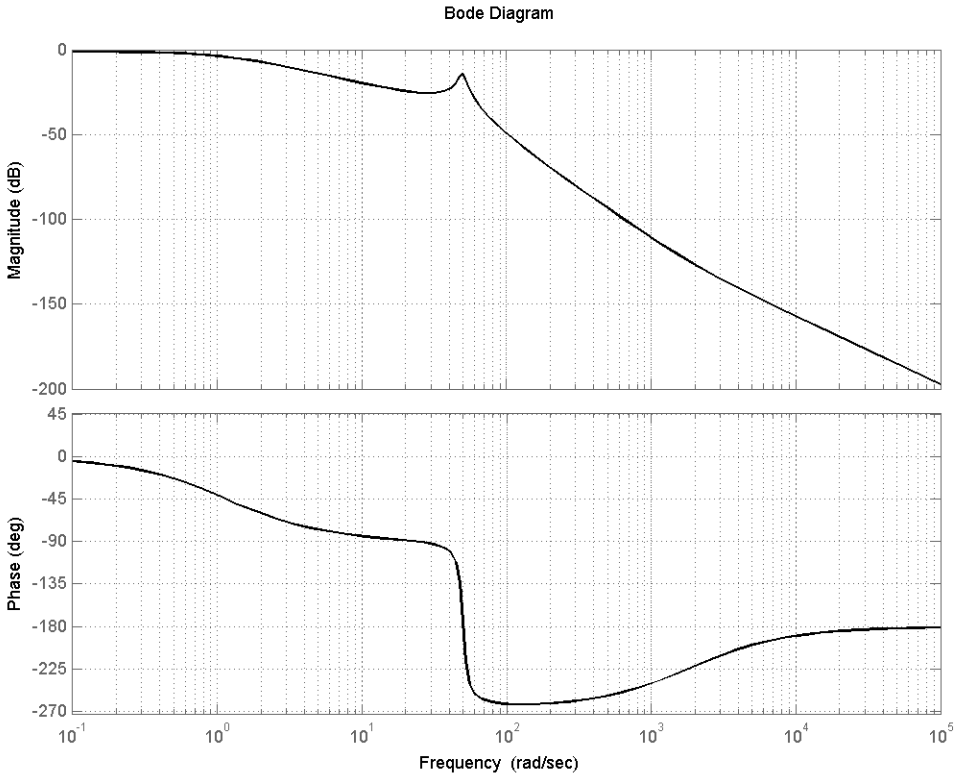

Fig. B.1. The Bode plot of the second order system ID for the acceleration system.

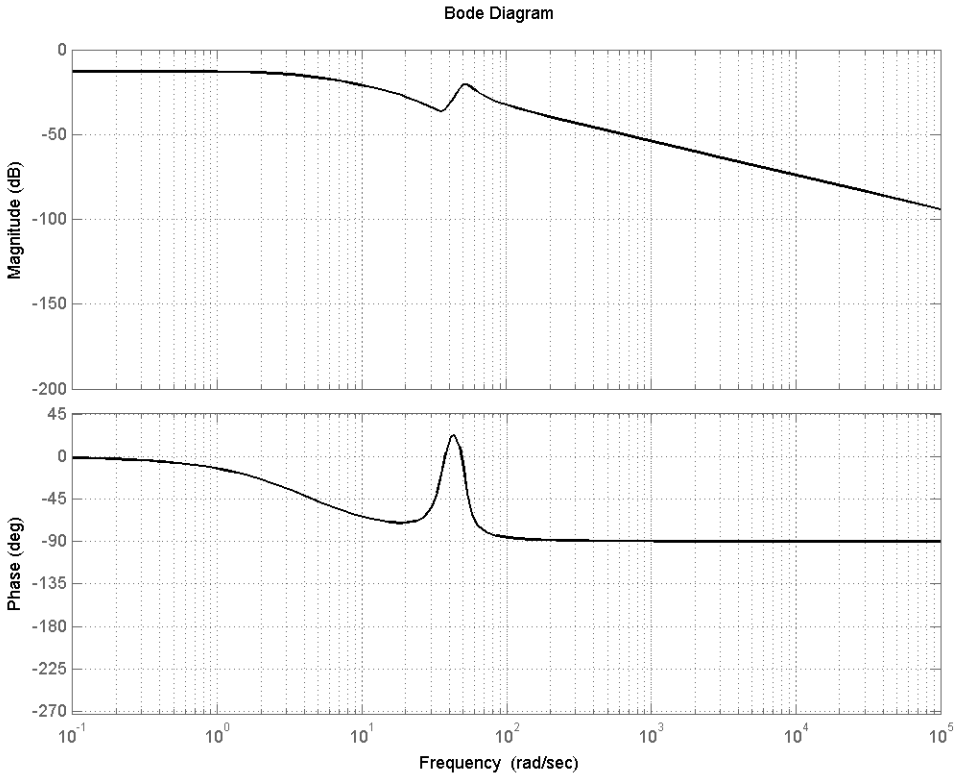

Fig. B.2. The Bode plot of the second order system ID for the brake system.

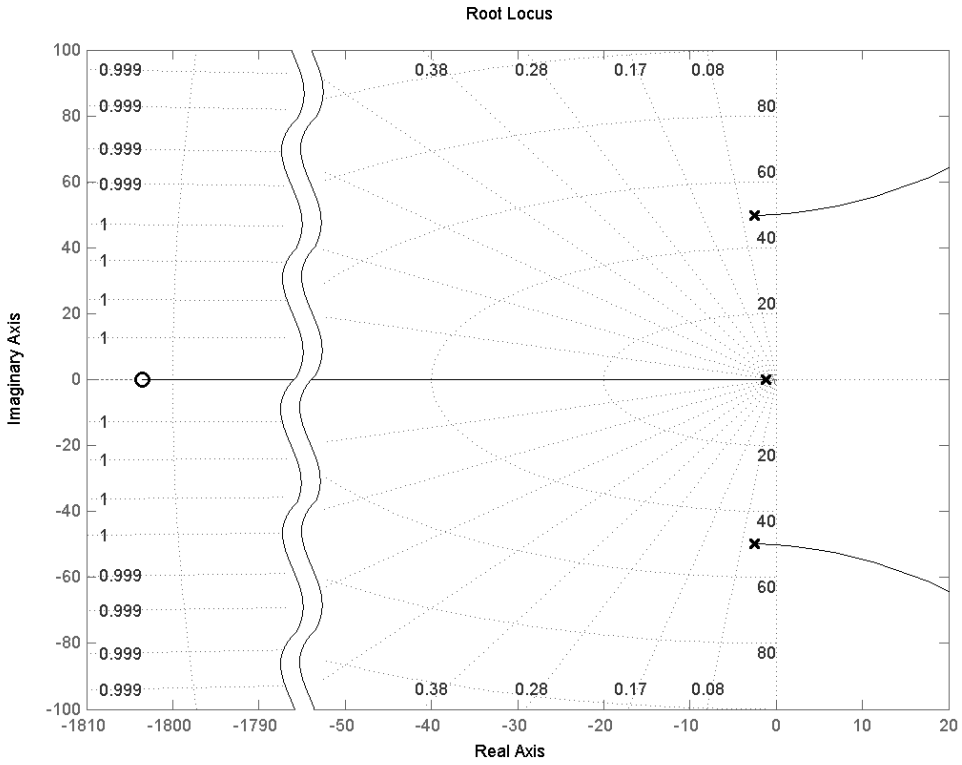

Fig. B.3. The root locus of the second order system ID for the acceleration system.

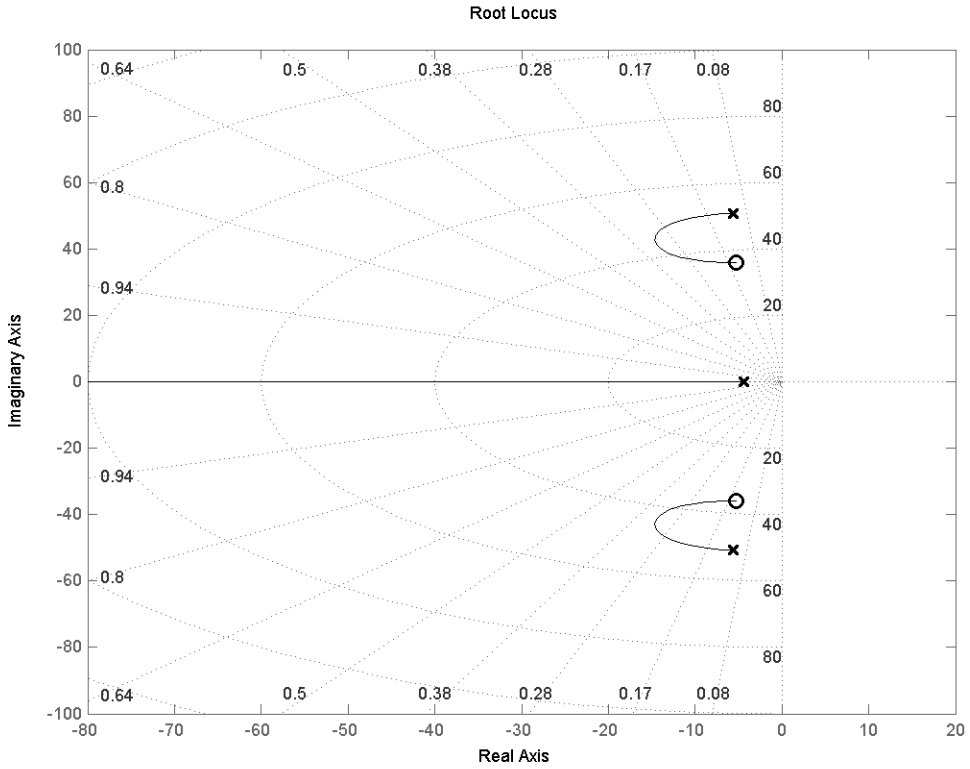

Fig. B.4. The root locus of the second order system ID for the brake system.

C. Stability Numerical Solution Code Example

A short program in MatLAB can calculate stable values of P_c and K_c for a given characteristic equation.

```
% eComp.m  -  Calculates stability of values of p and K for a uniformly
% corrupted plant compensator.
% by Alex Meadows
% 2/29/2012
uChange=0.4;    L=1+uChange;    G=1-uChange;
res=0.01;   max_K=2;    max_p=2;    index1=1;   index2=1;
goodchart.data=zeros(max_p/res+1,max_K/res+1);
goodchart.axis1=[0:res:max_K];  goodchart.axis2=[0:res:max_p];
for p=0:res:max_p
    for K=0:res:max_K
        ceq=[1 p+5.08 5.08*p+2503.7+1.383*K 2496.5*p+1803*K];
        q1=L*ceq(1)*ceq(4)-L*G*ceq(3)*ceq(2);
        q2=G*ceq(1)*ceq(4)-G*L*ceq(3)*ceq(2);
        q3=G*ceq(1)*ceq(4)-L*L*ceq(3)*ceq(2);
        q4=L*ceq(1)*ceq(4)-G*G*ceq(3)*ceq(2);
        state=(q1<0)*(q2<0)*(q3<0)*(q4<0);
        if state==0
            goodchart.data(index1,index2)=0;
        else
            goodchart.data(index1,index2)=1;
        end
        index1=index1+1;
    end
    index1=1;    index2=index2+1;
end
```

```
figure(1), surf(goodchart.axis1, goodchart.axis2, goodchart.data),...
        colormap([0.3 0.3 0.3; 1 1 1]),...
        xlabel('K_c'),ylabel('p_c'),zlabel('stable');
```